

Supporting Information

Imide-Functionalized Thiazole-Based Polymer Semiconductors: Synthesis, Structure-Property Correlations, Charge Carrier Polarity, and Thin-film Transistor Performance

Yongqiang Shi,^{†,‡,§} Han Guo,^{†,§} Minchao Qin,[§] Yuxi Wang,[†] Jiuyang Zhao,[†] Huiliang Sun,[†] Hang Wang,[†] Yulun Wang,[†] Xin Zhou,[†] Antonio Facchetti,[#] Xinhui Lu,^{*,§} Ming Zhou,[‡] Xugang Guo^{*,†}

[†] *Department of Materials Science and Engineering and The Shenzhen Key Laboratory for Printed Organic Electronics, Southern University of Science and Technology (SUSTech), No. 1088, Xueyuan Road, Shenzhen, Guangdong, 518055, China*

[‡] *School of Materials Science and Engineering, Southwest Petroleum University, Chengdu, Sichuan, 610500, China*

[§] *Department of Physics, The Chinese University of Hong Kong, New Territories, 999077, Hong Kong*

[#] *Department of Chemistry and the Materials Research Center, Northwestern University, Evanston, IL 60208, USA*

Table of Contents

1. Materials and Methods
2. Monomer and Polymer Synthesis
3. NMR Spectra of Monomers and Polymers
4. Single Crystal Structure Data
5. Polymer Thermal Properties
6. Polymer Optical and Electrochemical Properties
7. OTFT Fabrication and Characterization
8. GIWAXS Measurements and Data

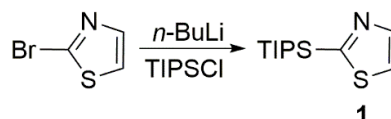
1. Materials and Methods.

All commercially available solvents, reagents, and chemicals were used as received without further purification unless otherwise stated. Anhydrous tetrahydrofuran and toluene were distilled from Na/benzophenone, and anhydrous dichloromethane and acetonitrile were distilled from CaH₂ under argon. 2,5-Bis(trimethylstannyl)thiophene, 3,4-difluoro-2,5-bis(trimethylstannyl)thiophene, and 2-bromothiazole were purchased from SunaTech Inc. (Suzhou, China). Hexabutyltin and methyl 5-bromothiazole-4-carboxylate were purchased from Adamas-bete® and Shuya Pharmaceutical Technology Co., Ltd (Shanghai, China), respectively. Unless otherwise stated, all operations and reactions were carried out under argon using standard Schlenk line techniques. Polymerizations were carried out on Initiator⁺ Microwave Synthesizer (Biotage, Sweden). Due to the high reactivity of some reactive reagents, such as n-BuLi and SOCl₂, their addition was carried out in a fume hood with excellent air circulation, and the sash was almost fully pulled down allowing only hands behind the sash glass during the operation. The addition of n-BuLi was completed using automatic injection pump with controllable addition rate. ¹H and ¹³C NMR spectra were recorded on a Bruker Ascend 400 and 500 MHz spectrometer, and the chemical shifts were referenced to residual protio-solvent signals. C, H, N, and S elemental analyses (EAs) of monomers and polymers were conducted at Shenzhen University (Shenzhen, China). Polymer molecular weights were characterized on Polymer Laboratories GPC-PL220 high temperature GPC/SEC system (Agilent Technologies) at 150 °C vs polystyrene standards using trichlorobenzene as the eluent. Differential scanning calorimetry (DSC) curves were recorded on Mettler STAR^e (TA Instrument) in nitrogen with a heating ramp of 10 °C min⁻¹, and thermogravimetric analysis (TGA) curves were collected on Mettler STAR^e (TA Instrument). UV-vis absorption spectra were recorded on a Shimadzu UV-3600 UV-VIS-NIR spectrophotometer. Cyclic voltammetry (CV)

measurements of polymer films were performed under argon atmosphere using a CHI760E voltammetric analyzer with 0.1 M tetra-*n*-butylammonium hexafluorophosphate in acetonitrile as the supporting electrolyte. A platinum disk working electrode, a platinum wire counter electrode, and a silver wire reference electrode were employed, and the ferrocene/ferrocenium (Fc/Fc⁺) was used as the internal reference for all measurements. The scanning rate was 100 mV s⁻¹. Polymer films were drop-casted from chloroform solutions on a Pt working electrode (2 mm in diameter). The supporting electrolyte solution was thoroughly purged with argon before all CV measurements. AFM measurements of polymer films were performed on a Dimension Icon Scanning Probe Microscope (Asylum Research, MFP-3D-Stand Alone) in tapping mode.

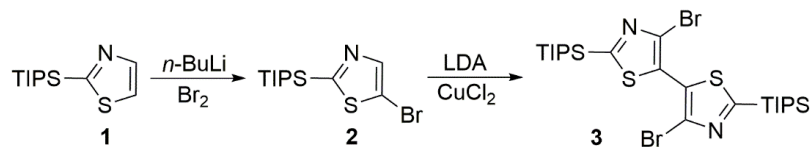
2. Monomer and Polymers Synthesis.

Synthesis of 2-(triisopropylsilyl)thiazole (**1**).^{1, 2}



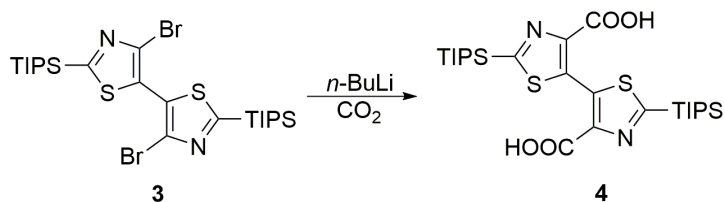
2-Bromothiazole (11.82 g, 72.0 mmol, 1 equiv) was added dropwise to *n*-BuLi (49.5 mL, 79.2 mmol, 1.1 equiv) in 190 mL of THF at -78 °C. The resulting solution was allowed to stir at this temperature for 1 h, and then triisopropylsilyltriflate (20.0 mL, 93.6 mmol, 1.3 equiv) was added dropwise. The solution was stirred at -78 °C for 1 h and then allowed to warm up to room temperature. The reaction was diluted with ethyl acetate, washed with saturated NaHCO₃, and brine, and then dried over anhydrous MgSO₄. After filtration, the reaction mixture was concentrated under a reduced pressure, and the residue was purified by flash column chromatography using petroleum ether as the eluent to give 2-triisopropylthiazole **1** (12.88 g, 74%). ¹H NMR (CDCl₃, 400 MHz) δ (ppm): 8.18 (d, 1H), 7.56 (d, 1H), 1.53 (sept, *J* = 7.2 Hz, 3H), 1.16 (d, *J* = 7.2 Hz, 18H); ¹³C NMR (CDCl₃, 100 MHz) δ (ppm): 169.78, 145.38, 121.03, 18.46, 11.67.

Synthesis of 2,2'-bis-triisopropylsilyl-4,4'-dibromo-5,5'-bithiazole (3).



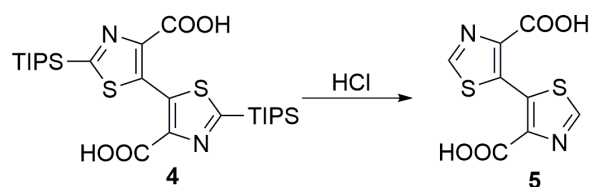
2-(Triisopropylsilyl)thiazole **1** (16.71 g, 69.2 mmol, 1 equiv) was dissolved in 300 mL anhydrous THF under N_2 and the solution was cooled to -78°C in an acetone/dry ice bath. n -Butyllithium (28.8 mL, 69.2 mmol, 1 equiv) was added dropwise to the reaction. The mixture became dark yellow and then precipitates formed. After stirring for 15 min, Br_2 (11.06 g, 69.2 mmol, 1 equiv) was added dropwise and a yellowish solution formed. To the reaction, LDA (38.1 mL, 76.1 mmol, 1.1 equiv) was then added dropwise and the reaction mixture was stirred for 10 min and anhydrous CuCl_2 (10.23 g, 76.1 mmol, 1.1 equiv) was added to the solution. After the CuCl_2 addition, the reaction mixture turned to brown color, and it was allowed to warm to room temperature after stirring for 2 h. The greenish reaction mixture was diluted with 150 mL hexanes and filtered through silica gel plug using hexanes as the eluent. The solvents were removed under reduced pressure and the residual crude product was recrystallized from ethanol. After filtration, the beige plates were obtained as the target product (15.4 g, 70%). The solvent was removed from the mother liquor and the residue was recrystallized from ethanol, and additional product was obtained (1.97 g, 9%) as the product. The combined overall yield for the reaction is 79%. ^1H NMR (CDCl_3 , 400 MHz) δ (ppm): 1.48 (sept, $J = 7.5$ Hz, 6H), 1.17 (d, 36H); ^{13}C NMR (CDCl_3 , 100 MHz) δ (ppm): 172.45, 130.31, 124.95, 18.44, 11.54.

Synthesis of 2,2'-Bis-triisopropylsilyl-4,4'-dicarboxylic acid-5,5'-bithiazole (4).



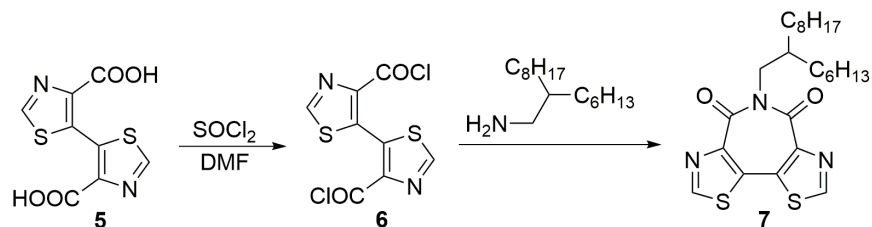
A solution of **3** (4.0 g, 6.26 mmol) in 60 mL anhydrous Et₂O was added dropwise to a stirring solution of *n*-BuLi (8.0 mL, 18.8 mmol) in 50 mL anhydrous Et₂O at -78 °C. After the addition, the reaction was then allowed to warm to room temperature for 1 h before bone dry CO₂ was bubbled into the reaction mixture for 1 h. The solvent was then evaporated under reduced pressure. To the residue was added 100 mL H₂O, acidified with 6 M HCl (aq), and filtered to afford a yellow solid, which was dried overnight in vacuum at 65 °C to afford the product compound **4** (yield: 95%).

Synthesis of 4,4'-dicarboxylic acid-5,5'-bithiazole (**5**).



A solution of **4** in diluted HCl and AcOH was heated to reflux for 3 h. The solvent was then evaporated under a reduced pressure and the residue was washed with CHCl₃ for 3 times to yield a brown solid **5** (yield: 99%), which can be used for the following reaction without further purification. ¹H NMR (400 MHz, DMSO) δ (ppm): 9.25 (s, 2H); ¹³C NMR (100 MHz, DMSO) δ (ppm): 162.50, 155.81, 145.45, 133.46.

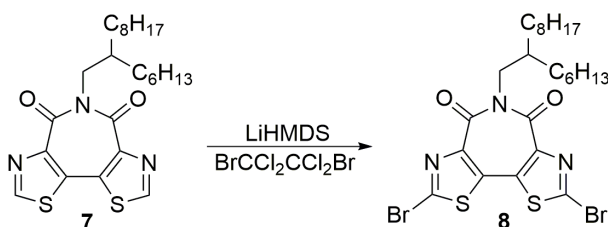
Synthesis of *N*-(2-hexyldecyl)-5,5'-bithiazole-4,4'-dicarboximide (**7**).



A mixture of compound **5** (0.88 g, 3.44 mmol) and SOCl₂ (20 mL) with 2 drops of dimethylformamide was heated to reflux for 8 h. The solvent was evaporated under reduced pressure to give compound **6**. Then a mixture of 2-hexyldecan-1-amine (0.25 g, 2.41 mmol) and

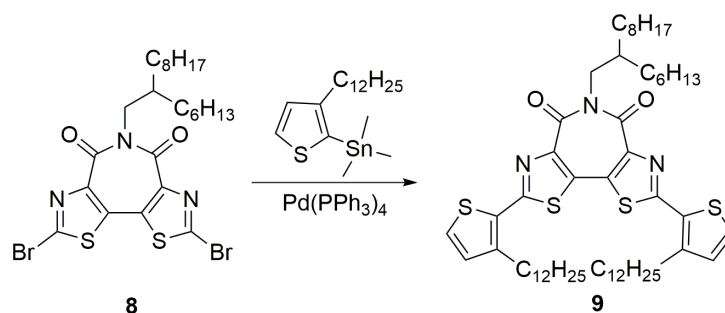
intermediate **6** was heated to 140 °C for 3 h under N₂. The crude product was further purified by column chromatography using petroleum ether:ethyl acetate (3:1 volume ratio) as the eluent to give a pale yellow solid **7** (yield: 27%). ¹H NMR (400 MHz, CDCl₃) δ (ppm): 8.91 (s, 2H), 4.35 (d, *J* = 7.2 Hz, 2H), 2.04-1.95 (m, 1H), 1.26 (b, 24H), 0.88 (q, *J* = 6.8 Hz, 6H). ¹³C NMR (100 MHz, CDCl₃) δ (ppm): 160.26, 152.74, 146.59, 129.94, 50.44, 36.33, 31.93, 31.87, 31.71, 30.03, 29.71, 29.61, 29.33, 26.43, 26.39, 22.69, 22.67, 14.16.

Synthesis of *N*-(2-hexyldecyl)-2,2'-dibromo-5,5'-bithiazole-4,4'-dicarboximide (8**).**



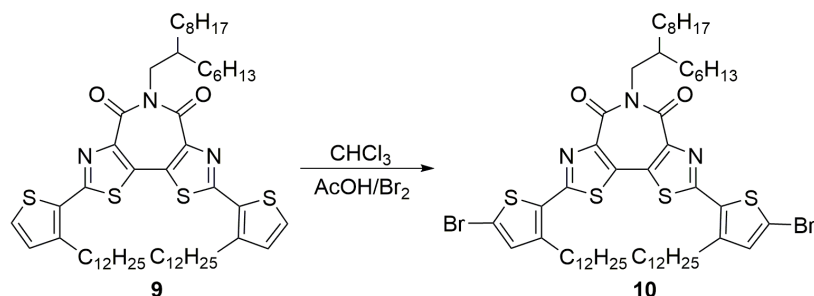
The imide **7** (184 mg, 0.57 mmol) and BrCCl₂CCl₂Br (464 mg, 1.43 mmol) was dissolved in anhydrous THF. lithium hexamethyldisilazide (LiHMDS) (1.54 mL, 2.0 mmol) was added dropwise at -78 °C and stirred at this temperature for 20 min under N₂. Then to the reaction was added saturated NH₄Cl aqueous solution. The aqueous phase was extracted with dichloromethane for 3 times and the combined organic phase was evaporated under reduced pressure to afford a yellow solid, which was further purified by column chromatography using petroleum ether:ethyl acetate (5:1 volume ratio) as the eluent and then recrystallized from isopropanol (yield: 45%). ¹H NMR (400 MHz, CDCl₃) δ (ppm): 4.29 (d, *J* = 7.1 Hz, 2H), 1.99-1.90 (m, 1H), 1.25 (b, 24H), 0.88 (dd, *J* = 12.1, 6.8 Hz, 6H). ¹³C NMR (100 MHz, CDCl₃) δ (ppm): 158.77, 145.75, 136.86, 131.87, 50.84, 36.31, 31.94, 31.87, 31.70, 30.03, 29.71, 29.61, 29.34, 26.41, 26.38, 22.71, 22.68, 14.16.

Synthesis of *N*-(2-hexyldecyl)-2,2'-bis(3-dodecylthiophene-2-yl)-5,5'-bithiazole-4,4'-dicarboximide (9**).**



The dibrominated imide **8** (206 mg, 0.33 mmol), 2-trimethyltin-3-dodecylthiophene (414 mg, 0.99 mmol), Pd(PPh₃)₄ (20 mg, 0.016 mmol), and 3 mL DMF were combined, and the reaction mixture was stirred under microwave irradiation at 150 °C for 3 h. The solvent was then removed under reduced pressure to afford a red solid, which was further purified by column chromatography over silica gel using CH₂Cl₂:Hexane (1:1 volume ratio) mixed solvent as the eluent to afford an orange solid as the product **9** (yield: 30%). ¹H NMR (400 MHz, CDCl₃) δ (ppm): 7.45 (d, *J* = 5.1 Hz, 2H), 7.03 (d, *J* = 5.1 Hz, 2H), 4.36 (d, *J* = 7.2 Hz, 2H), 3.00 (t, *J* = 7.6 Hz, 4H), 2.10-2.01 (m, 1H), 1.76 (dt, *J* = 15.2, 7.6 Hz, 4H), 1.27 (b, 60H), 0.88 (q, *J* = 6.6 Hz, 12H). ¹³C NMR (100 MHz, CDCl₃) δ (ppm): 160.25, 159.67, 145.46, 145.05, 130.68, 129.99, 129.08, 128.74, 50.76, 36.34, 31.94, 31.90, 31.75, 30.13, 30.08, 29.95, 29.80, 29.70, 29.62, 29.54, 29.50, 29.39, 26.45, 22.71, 14.14.

Synthesis of *N*-(2-hexyldecyl)-2,2'-bis(5-bromo-3-dodecylthiophene-2-yl)-5,5'-bithiazole-4,4'-dicarboximide (10**).**



Br₂ (118 mg, 0.74 mmol) was added to a solution of **9** (238 mg, 0.25 mmol) in CHCl₃:AcOH (5:1; total volume: 6 mL) in one portion. The reaction mixture was stirred at room temperature for 4 h,

and 30 mL H₂O was then added. Next, the reaction mixture was extracted with 30 mL CH₂Cl₂ for 3 times, and the combined organic layer was washed with 50 mL brine and then dried over anhydrous MgSO₄. After filtration, the solvent was removed under reduced pressure to afford an orange solid, which was purified by column chromatography over silica gel with CH₂Cl₂:Hexane (1:2 volume ratio) as the eluent. The compound **10** was obtained as an orange solid (yield: 70%). ¹H NMR (400 MHz, CDCl₃) δ (ppm): 7.29 (s, 2H), 4.33 (d, *J* = 7.1 Hz, 2H), 2.91 (t, *J* = 7.6 Hz, 4H), 2.02 (s, 1H), 1.79-1.67 (m, 4H), 1.28 (b, 60H), 0.89 (t, *J* = 6.2 Hz, 12H). ¹³C NMR (100 MHz, CDCl₃, ppm) δ (ppm): 160.25, 158.19, 145.49, 145.29, 133.35, 131.66, 128.62, 117.62, 50.76, 36.38, 31.96, 30.13, 29.72, 30.13, 29.58, 29.47, 29.39, 22.71, 14.14. Anal. Calcd. for C₅₆H₈₅Br₂N₃O₂S₄(%); C, 60.03; H, 7.65; N, 3.75; S, 11.45. Found (%): C, 60.22; H, 7.55; N, 3.65; S, 11.57.

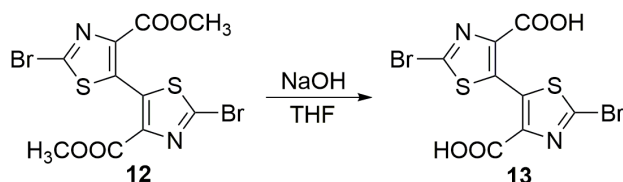
Synthesis of dimethyl 2,2'-dibromo-bis-5,5'-thiazole-4,4'-dicarboxylate (**12**)



Methyl 2-bromothiazole-4-carboxylate (200 mg, 0.9 mmol), PdCl₂(PhCN)₂ (34 mg, 0.09 mmol), and DMSO (10 mL) were added to a 20 mL Schlenk tube equipped with a magnetic stirring bar. AgF (228 mg, 1.8 mmol) was added in one portion and the resulting mixture was heated and stirred at 60 °C for 3 h. Additional AgF was then added and stirring was continued for another 3 h. The reaction solution was poured into 100 mL H₂O and extracted with 100 mL CH₂Cl₂ for 3 times. The combined organic layer was dried over MgSO₄, and the solvent was evaporated under reduced pressure. The crude product was further purified by column chromatography on silica gel using petroleum ether:ethyl acetate (3:1 volume ratio) as the eluent to give compound **12** as a white solid

(yield: 40%). ^1H NMR (400 MHz, CDCl_3) δ (ppm): 3.88 (s, 6H). ^{13}C NMR (100 MHz, CDCl_3) δ (ppm): 160.27, 143.84, 138.15, 135.10, 52.94.

Synthesis of 2,2'-dibromo-bis-5,5'-thiazole-4,4'-dicarboxylic acid (**13**).³



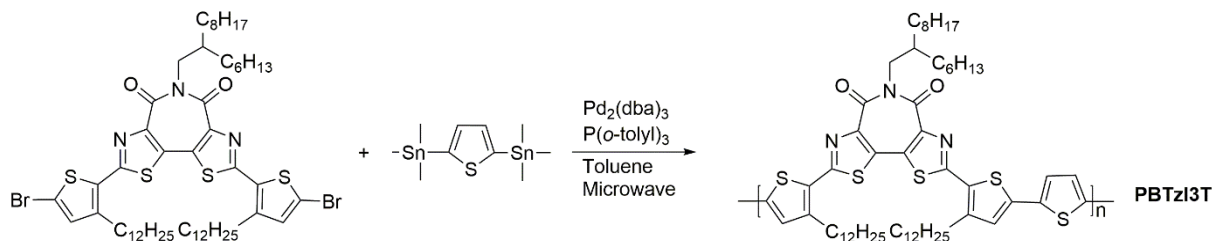
A mixture of compound **12** (900 mg, 2.03 mmol) and sodium hydroxide (330 mg, 8.14 mmol) in THF:water (20 mL:5 mL) was refluxed overnight. The solvent was removed under reduced pressure to 1/4 of its original volume. 50 mL H_2O was added to the solution and the resulting mixture was treated with dilute HCl. The precipitate was filtered and washed with H_2O for 3 times to give product compound **13** (98%). ^{13}C NMR (126 MHz, DMSO) δ (ppm): 161.27, 145.37, 137.91, 135.47.

General Procedure for Polymerizations via Stille Coupling for the Synthesis of Polymers

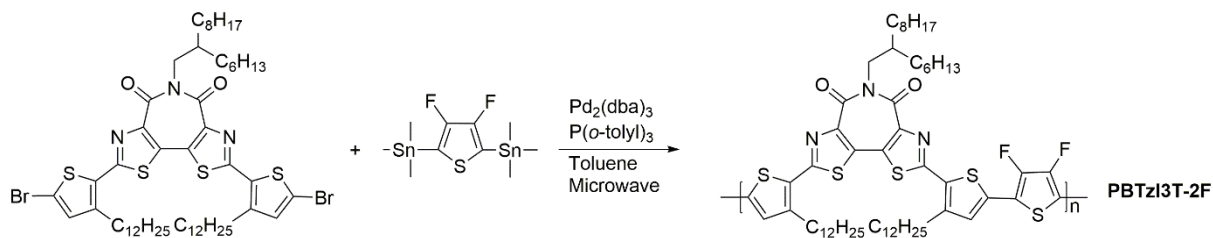
PBTzI3T, PBTzI3T-2F, PDTzTIT, PDTzTIT-2F, PDTzTI and PBTzI.

To a flame-dried glass tube was charged with two monomers (0.1 mmol each), tris(dibenzylideneacetone)dipalladium (0) ($\text{Pd}_2(\text{dba})_3$), and tris(*o*-tolyl)phosphine ($\text{P}(\text{o-tolyl})_3$) (1:8, $\text{Pd}_2(\text{dba})_3$: $\text{P}(\text{o-tolyl})_3$ molar ratio; Pd loading: 0.03-0.05 equiv). The tube and its contents were subjected to 3 pump/purge cycles with argon, followed by the addition of 3 mL anhydrous toluene via syringe. The tube was sealed under argon flow and then stirred at 80 °C for 10 min, 100 °C for 10 min, and 140 °C for 3 h under microwave irradiation. Then, 0.1 mL 2-(tributylstanny)thiophene was added and the reaction mixture was stirred under microwave irradiation at 140 °C for 0.5 h. Finally, 0.2 mL 2-bromothiophene was added and the reaction mixture was stirred at 140 °C for another 0.5 h. After cooling to room temperature, the reaction mixture was slowly dripped into 100 mL methanol, containing 5 mL 12 N hydrochloric acid, under vigorous stirring. After stirring for

1 h, the solid precipitate was transferred to a Soxhlet thimble. After drying, the crude product was subjected to sequential Soxhlet extraction with the solvent sequence depending on the solubility of the particular polymer. After final extraction, the polymer solution was concentrated to ~20 mL, and then dripped into 100 mL methanol under vigorous stirring. The polymer was collected by filtration and dried under reduced pressure to afford a deep colored solid as the final product.

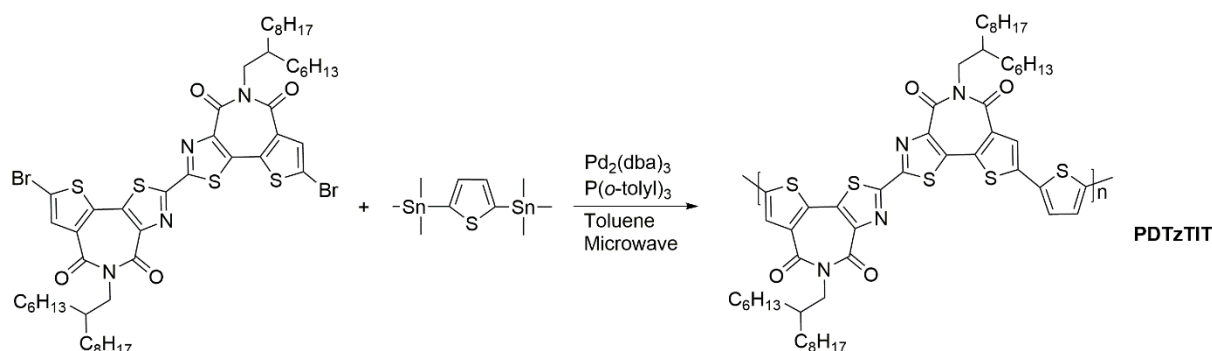


PBTzI3T. The solvent sequence for Soxhlet extraction was methanol, acetone, hexane, dichloromethane, and chloroform. The chloroform fraction was concentrated by removing most of solvent and precipitated into methanol. The solid was collected by filtration and dried in vacuum to afford the polymer as a deep colored solid (yield: 53%). ^1H NMR (400 MHz, CCl_4D_2 , 120 °C) δ (ppm): 7.67 (s, 2H), 7.37 (d, 2H), 4.39 (d, 2H), 3.05 (t, 4H), 2.10 (s, 1H), 1.79 (m, 4H), 1.35 (m, 60H), 0.95 (m, 12H). $M_n = 24$ kDa, PDI = 1.7. Anal. Calcd. for $\text{C}_{60}\text{H}_{87}\text{N}_3\text{O}_2\text{S}_5$ (%): C, 69.11; H, 8.41; N, 4.03; S, 15.38. Found (%): C, 68.98; H, 8.32; N, 4.33; S, 15.21.

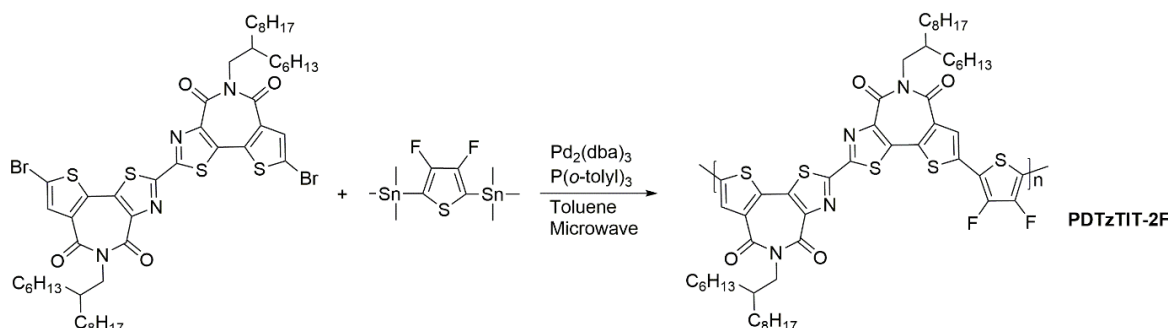


PBTzI3T-2F. The solvent sequence for Soxhlet extraction was methanol, acetone, hexane, dichloromethane, and chloroform. The chloroform fraction was concentrated by removing most of solvent and precipitated into methanol. The solid was collected by filtration and dried in vacuum to afford the polymer as a deep colored solid (yield: 62%). ^1H NMR (400 MHz, CCl_4D_2 , 120 °C)

δ (ppm): 7.29 (s, 2H), 4.33 (d, 2H), 2.91 (t, 4H), 2.02 (s, 1H), 1.79-1.67 (m, 4H), 1.28 (b, 60H), 0.89 (t, 12H). M_n = 11 kDa, PDI = 1.2. Anal. Calcd. for $C_{60}H_{85}F_2N_3O_2S_5$ (%): C, 66.81; H, 7.94; N, 3.90; S, 14.86. Found (%): C, 66.69; H, 7.82; N, 3.69; S, 14.56.

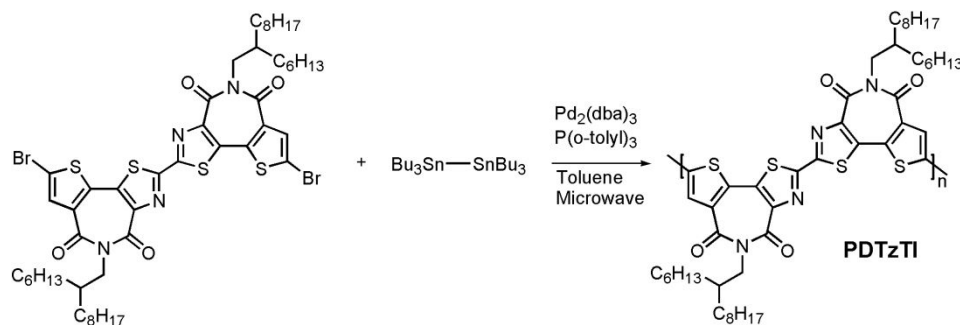


PDTzTIT. The solvent sequence for Soxhlet extraction was methanol, acetone, hexane, dichloromethane, and chloroform. The chloroform fraction was concentrated by removing most of solvent under reduced pressure and precipitated into methanol. The solid was collected by filtration and dried in vacuum to afford the polymer as a deep colored solid (yield: 72%). 1H NMR (400 MHz, CCl_4D_2 , 120 °C) δ (ppm): 7.58 (s, 2H), 7.16 (s, 2H), 4.29 (d, 4H), 1.99-1.92 (m, 2H), 1.44-1.19 (m, 48H), 0.89 (d, 12H). M_n = 20 kDa, PDI = 1.8. Anal. Calcd. for $C_{54}H_{70}N_4O_4S_5$ (%): C, 64.89; H, 7.06; N, 5.61; S, 16.04. Found (%): C, 64.33; H, 7.06; N, 5.08; S, 15.33.

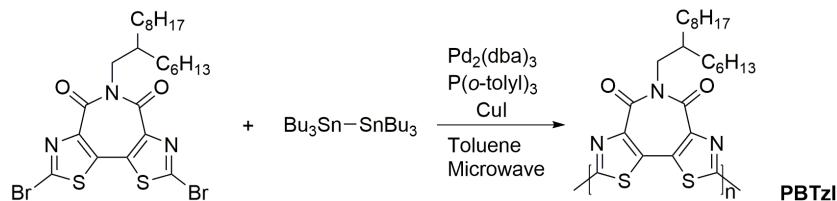


PDTzTIT-2F. The solvent sequence for Soxhlet extraction was methanol, acetone, hexane, dichloromethane, and chloroform. The chloroform fraction was concentrated by removing most of solvent and precipitated into methanol. The solid was collected by filtration and dried in vacuum

to afford the polymer as a deep colored solid (70%). ^1H NMR (400 MHz, CCl_4D_2 , 120 $^\circ\text{C}$) δ : 7.82 (s, 2H), 4.29 (d, 4H), 1.99-1.92 (m, 2H), 1.44-1.19 (m, 48H), 0.96 (d, 12H). $M_n = 14$ kDa, PDI = 1.2. Anal. Calcd. for $\text{C}_{54}\text{H}_{68}\text{F}_2\text{N}_4\text{O}_4\text{S}_5$ (%): C, 62.64; H, 6.62; N, 5.41; S, 15.48. Found (%): C, 62.94; H, 6.62; N, 5.22; S, 15.29.



PDTzTI. The solvent sequence for Soxhlet extraction was methanol, acetone, hexane, and dichloromethane. The dichloromethane fraction was concentrated by removing most of solvent and precipitated into methanol. The solid was collected by filtration and dried in vacuum to afford the polymer as a deep colored solid (86%). ^1H NMR (400 MHz, CDCl_3 , 120 $^\circ\text{C}$) δ : 7.81 (s, 2H), 4.37 (d, 4H), 2.09 (m, 2H), 1.38 (m, 48H), 0.96 (d, 12H). $M_n = 7.0$ kDa, PDI = 1.1. Anal. Calcd for $\text{C}_{50}\text{H}_{68}\text{N}_4\text{O}_4\text{S}_4$ (%): C, 65.46; H, 7.47; N, 6.11; S, 13.98. Found (%): C, 65.28; H, 7.39; N, 5.88; S, 13.97.



PBTzI. A glass tube was charged with two monomers (0.1 mmol each), tris(dibenzylideneacetone)dipalladium (0) ($\text{Pd}_2(\text{dba})_3$), and tris(*o*-tolyl)phosphine ($\text{P}(\text{o-tolyl})_3$) (1:8, $\text{Pd}_2(\text{dba})_3$: $\text{P}(\text{o-tolyl})_3$ molar ratio; Pd loading: 0.03-0.05 equiv; CuI: 0.01 equiv). The tube and its contents were subjected to 3 pump/purge cycles with argon, followed by the addition of 3 mL anhydrous toluene via syringe. The solvent sequence for Soxhlet extraction was methanol, acetone,

hexane, and dichloromethane. The dichloromethane fraction was concentrated by removing most of solvent under reduced pressure and precipitated into methanol. The solid was collected by filtration and dried in vacuum to afford the polymer as a deep colored solid (80%). ^1H NMR (400 MHz, CCl_4D_2 , 120 $^\circ\text{C}$) δ (ppm): 3.70 (d, 2H), 1.37 (m, 1H), 0.64 (b, 24H), 0.23 (b, 6H). $M_n = 5.8$ kDa, PDI = 2.6. Anal. Calcd. for $\text{C}_{24}\text{H}_{33}\text{N}_3\text{O}_2\text{S}_2$ (%): C, 46.53; H, 5.37; N, 6.78; S, 10.35. Found (%): C, 46.57; H, 5.40; N, 6.88; S, 10.37.

3. NMR Spectra of Monomers and Polymers.

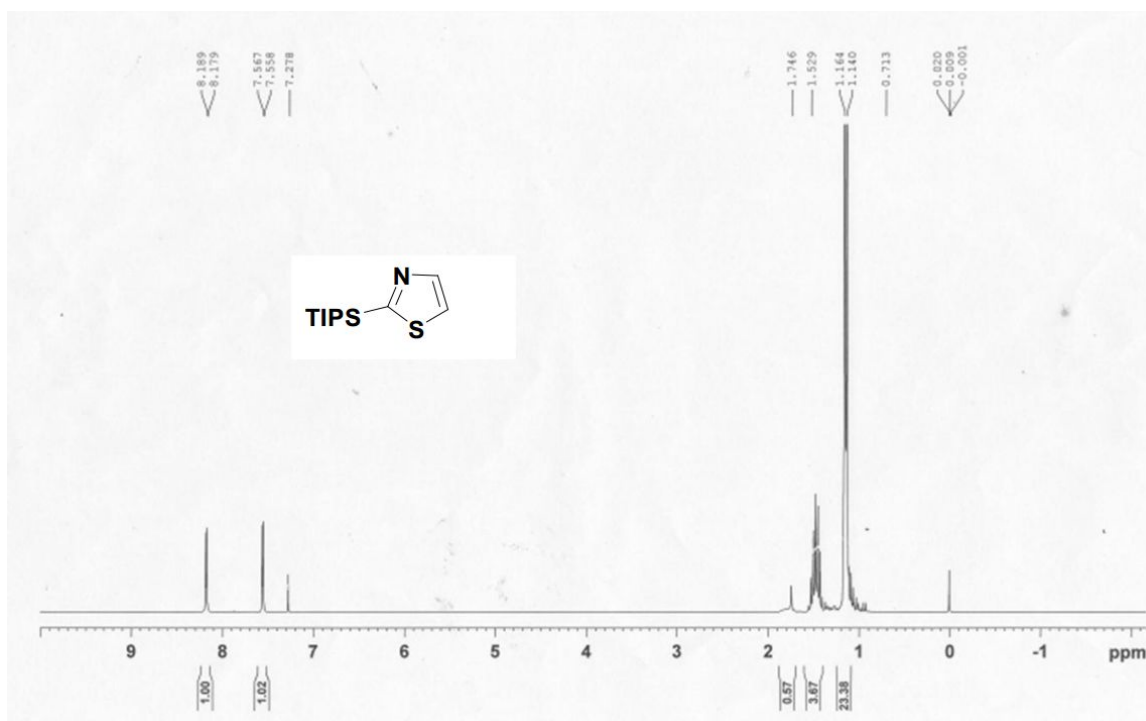


Figure S1. ^1H NMR spectrum of compound **1** (400 M, r.t., in CDCl_3).

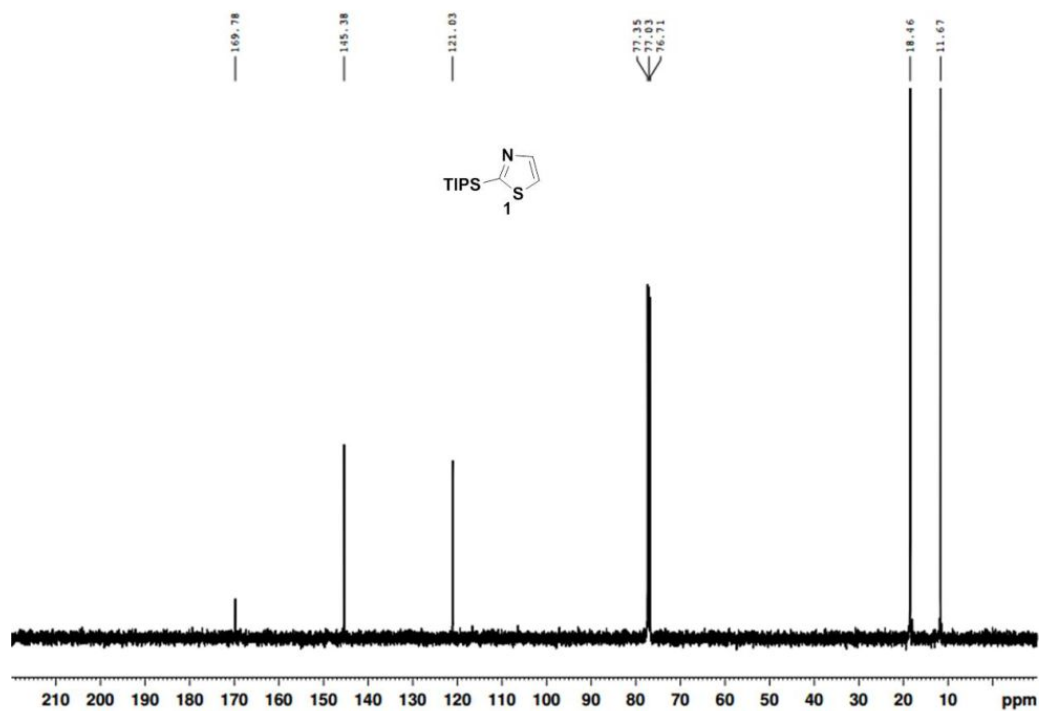


Figure S2. ^{13}C NMR spectrum of compound **1** (100 M, r.t., in CDCl_3).

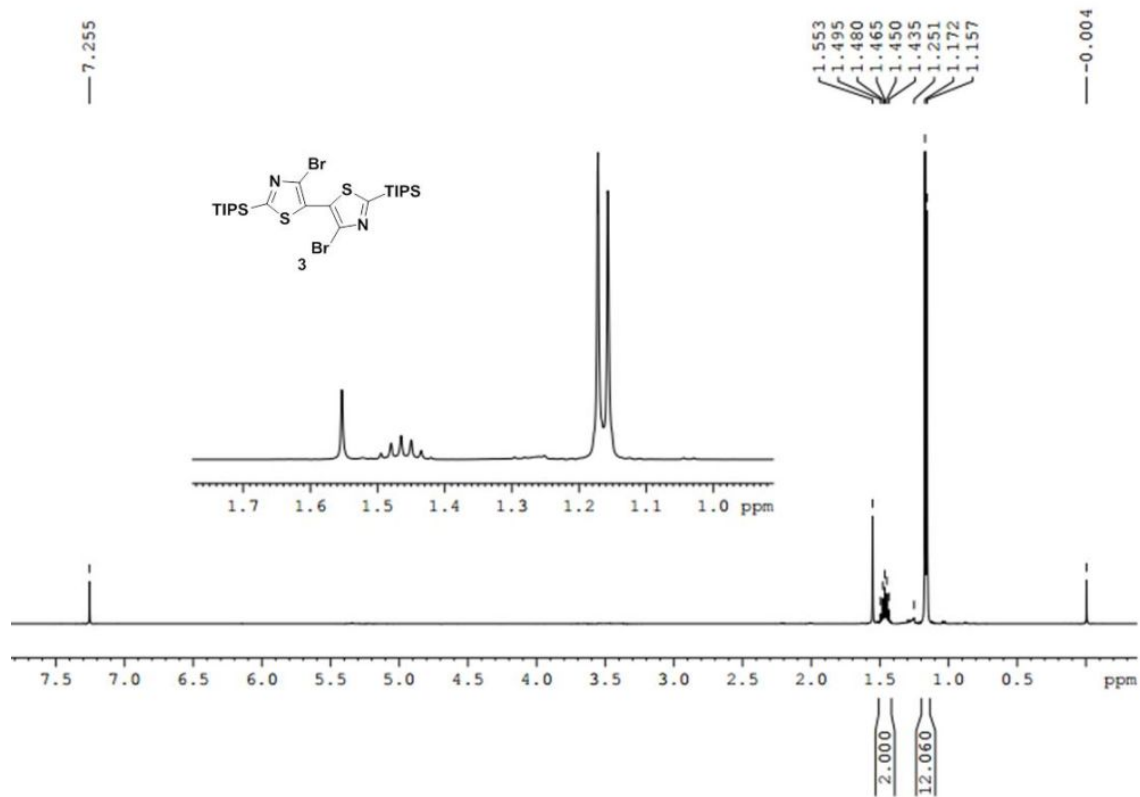


Figure S3. ¹H NMR spectrum of compound **3** (400 M, r.t., in CDCl₃).

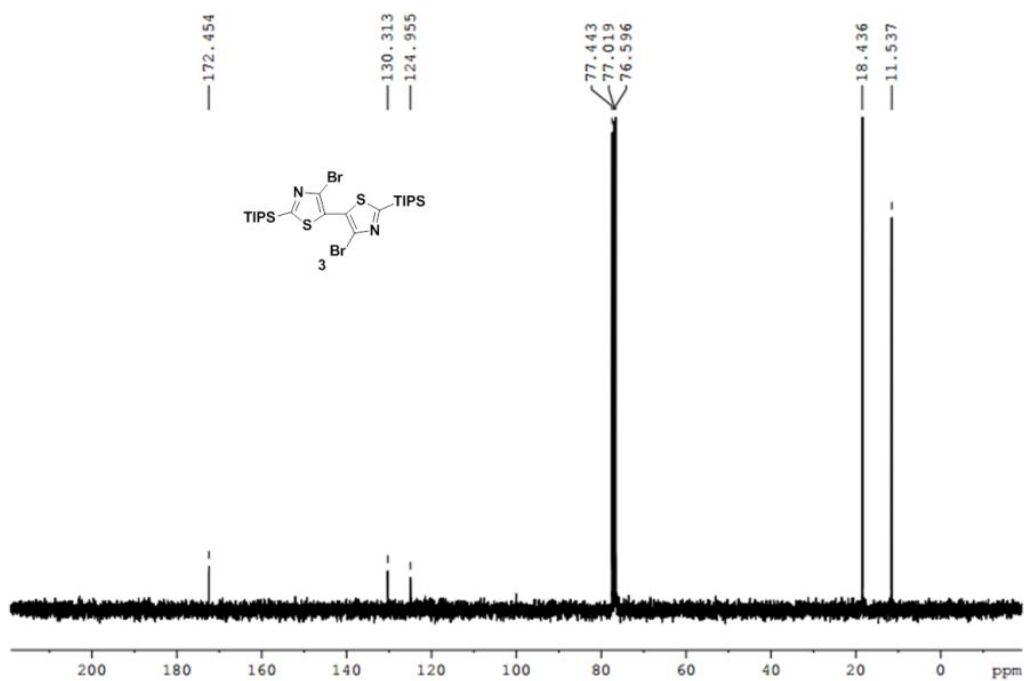


Figure S4. ^{13}C NMR spectrum of compound **3** (100 M, r.t., in CDCl_3).

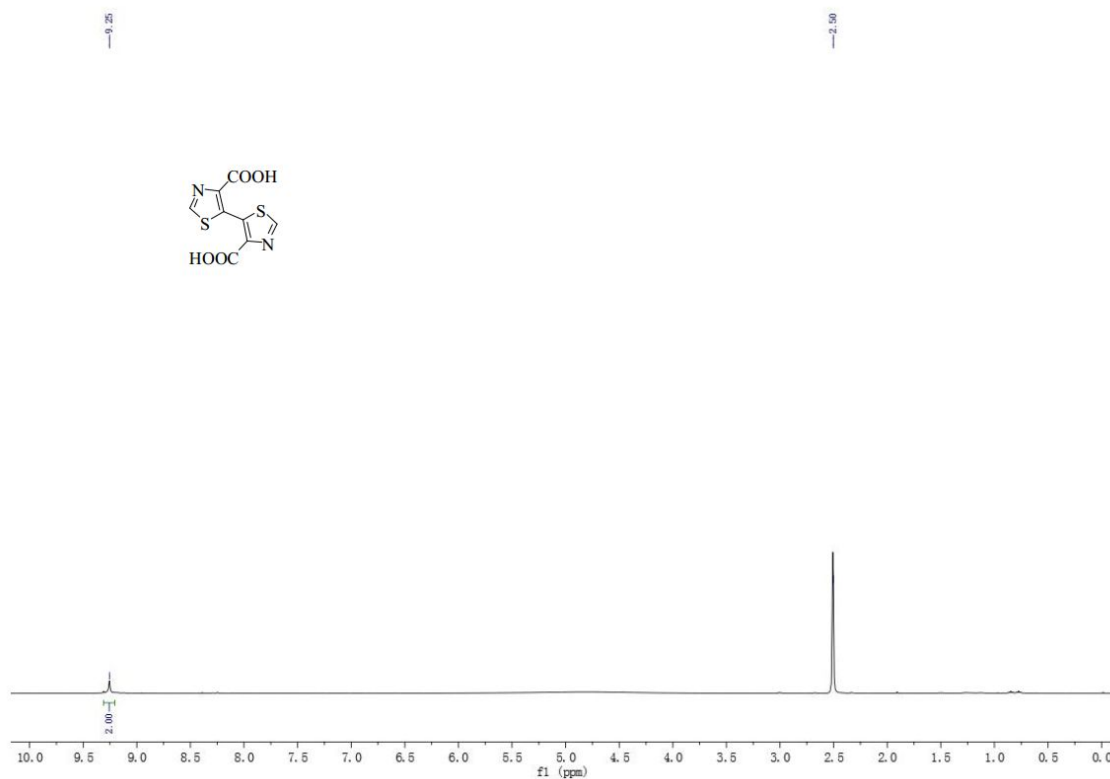


Figure S5. ^1H NMR spectrum of compound **5** (400 M, r.t., in DMSO).

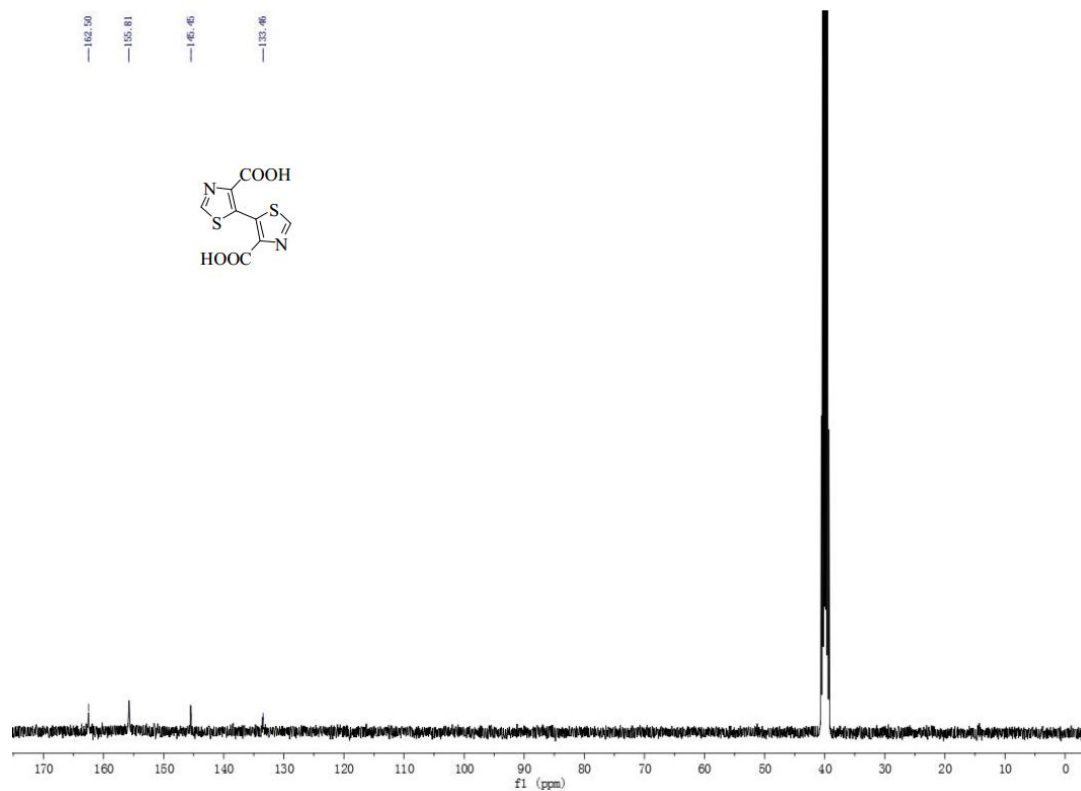


Figure S6. ¹³C NMR spectrum of compound **5** (100 M, r.t., in DMSO).

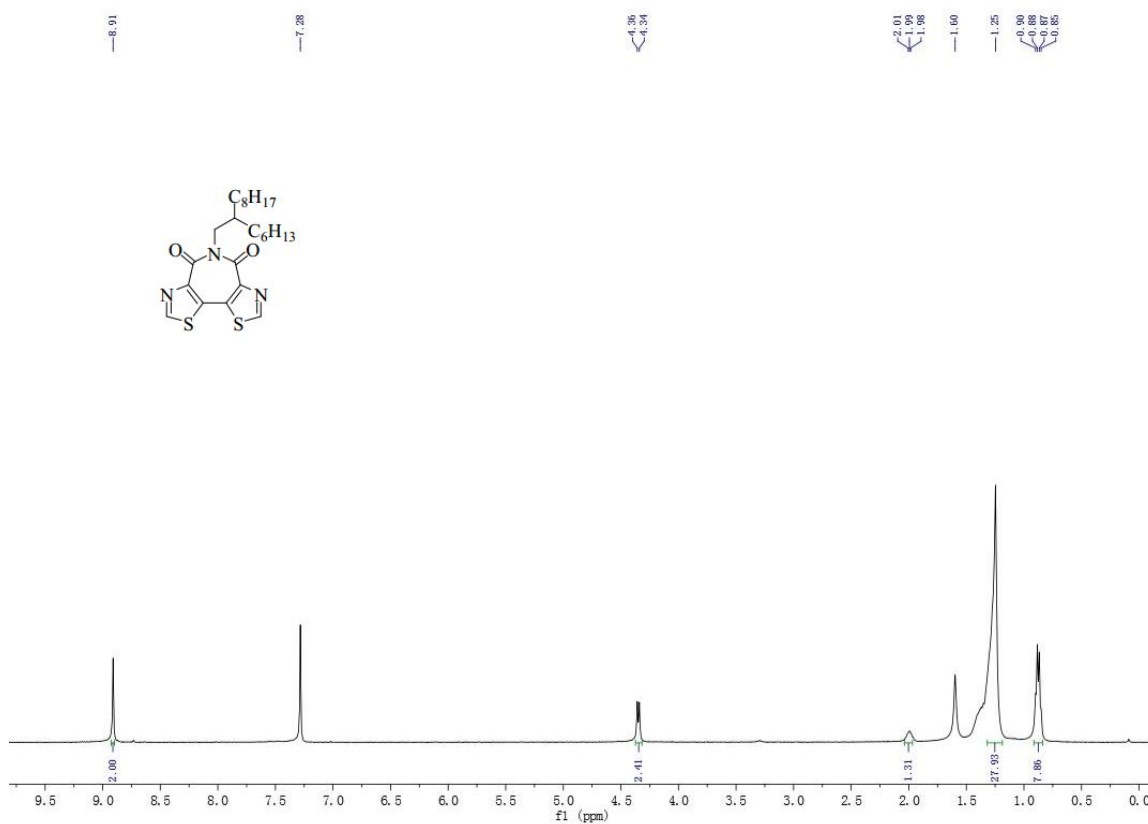


Figure S7. ^1H NMR spectrum of **7** (400 M, r.t., in CDCl_3).

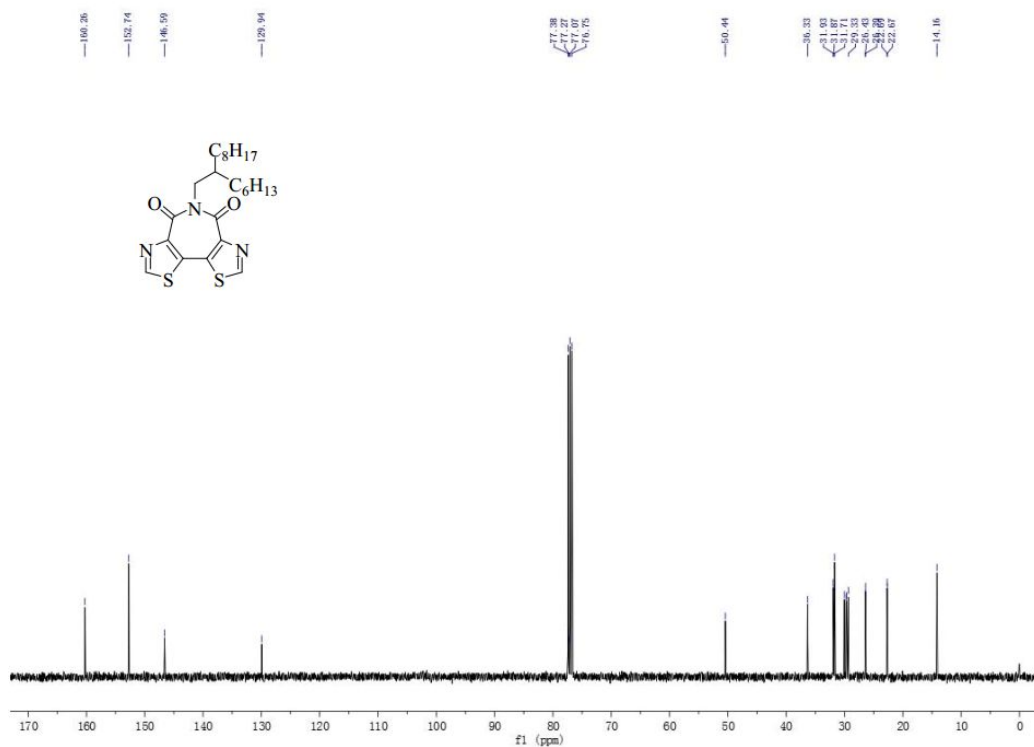


Figure S8. ^{13}C NMR spectrum of **7** (100 M, r.t., in CDCl_3).

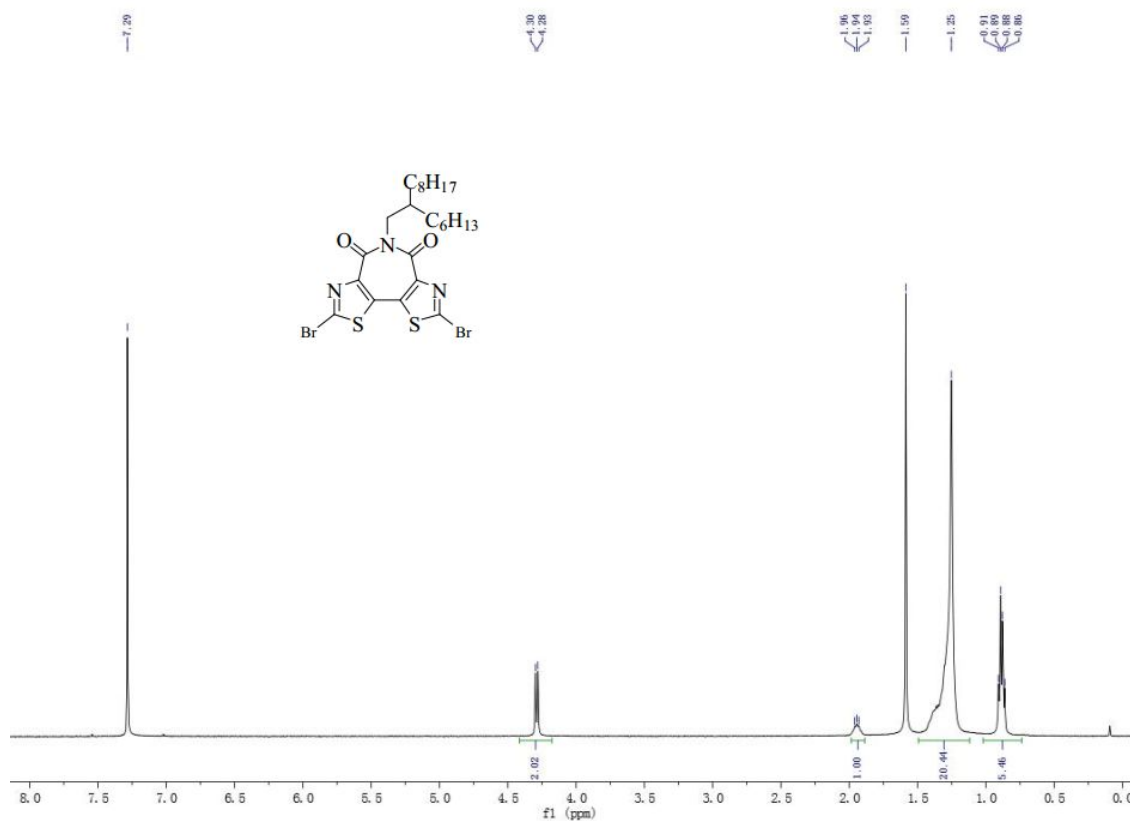


Figure S9. ¹H NMR spectrum of compound **8** (400 M, r.t., in CDCl₃).

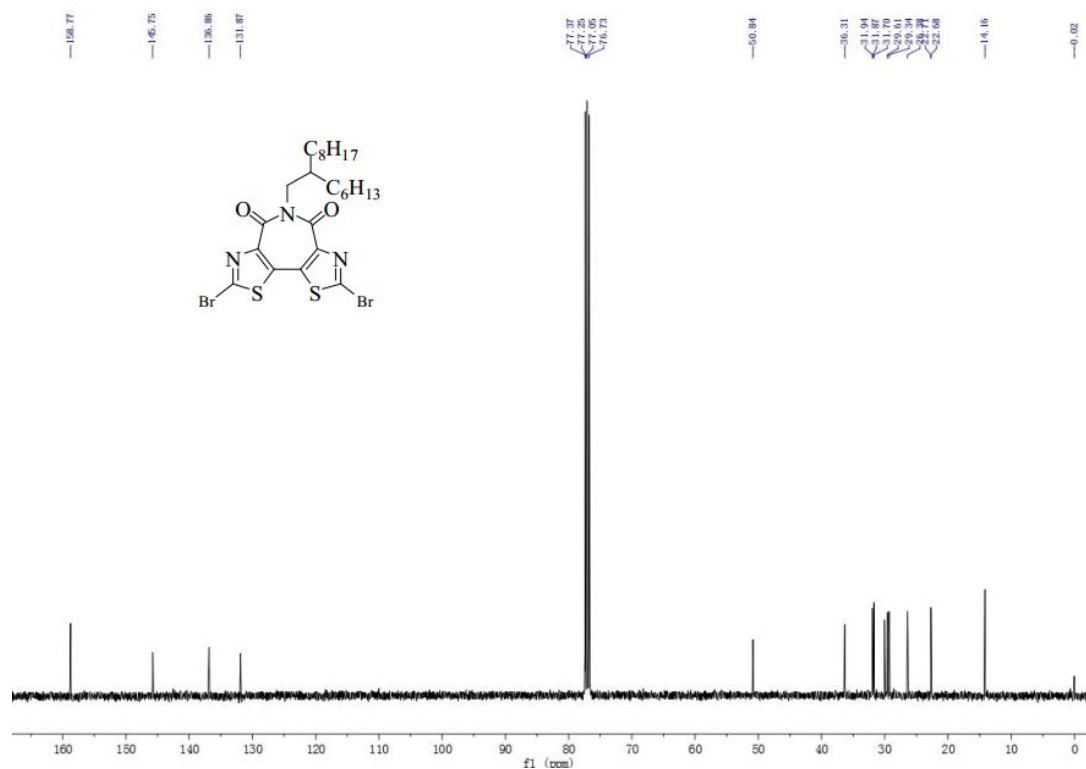


Figure S10. ¹³C NMR spectrum of compound **8** (100 M, r.t., in CDCl₃).

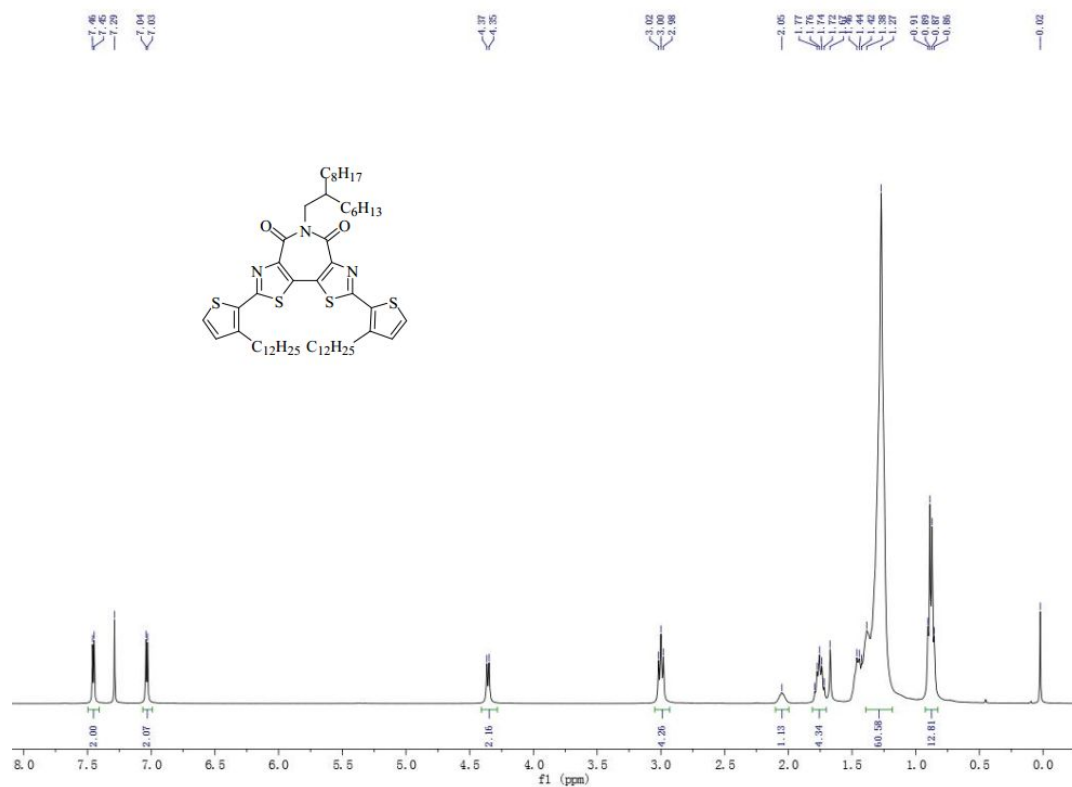


Figure S11. ¹H NMR spectrum of compound **9** (400 M, r.t., in CDCl₃).

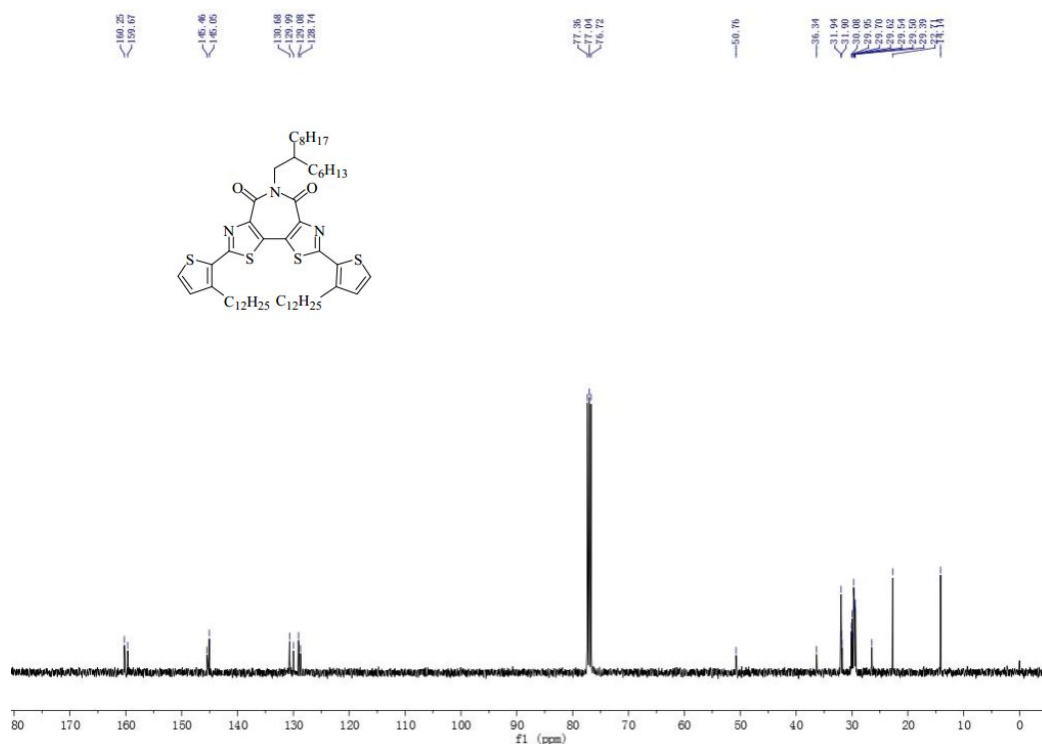


Figure S12. ^{13}C NMR spectrum of compound **9** (100 M, r.t., in CDCl_3).

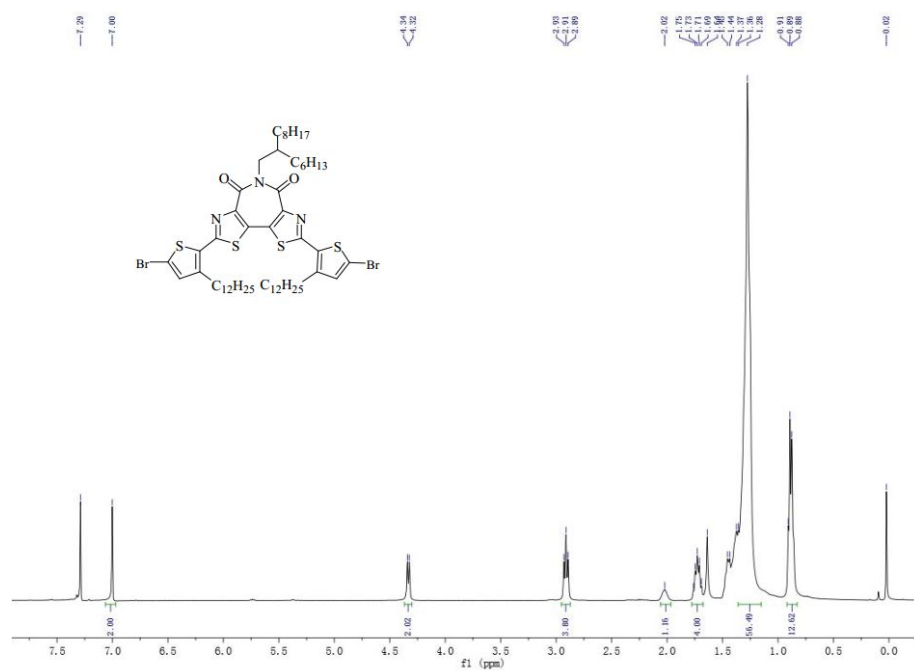


Figure S13. ^1H NMR spectrum of compound **10** (400 M, r.t., in CDCl_3).

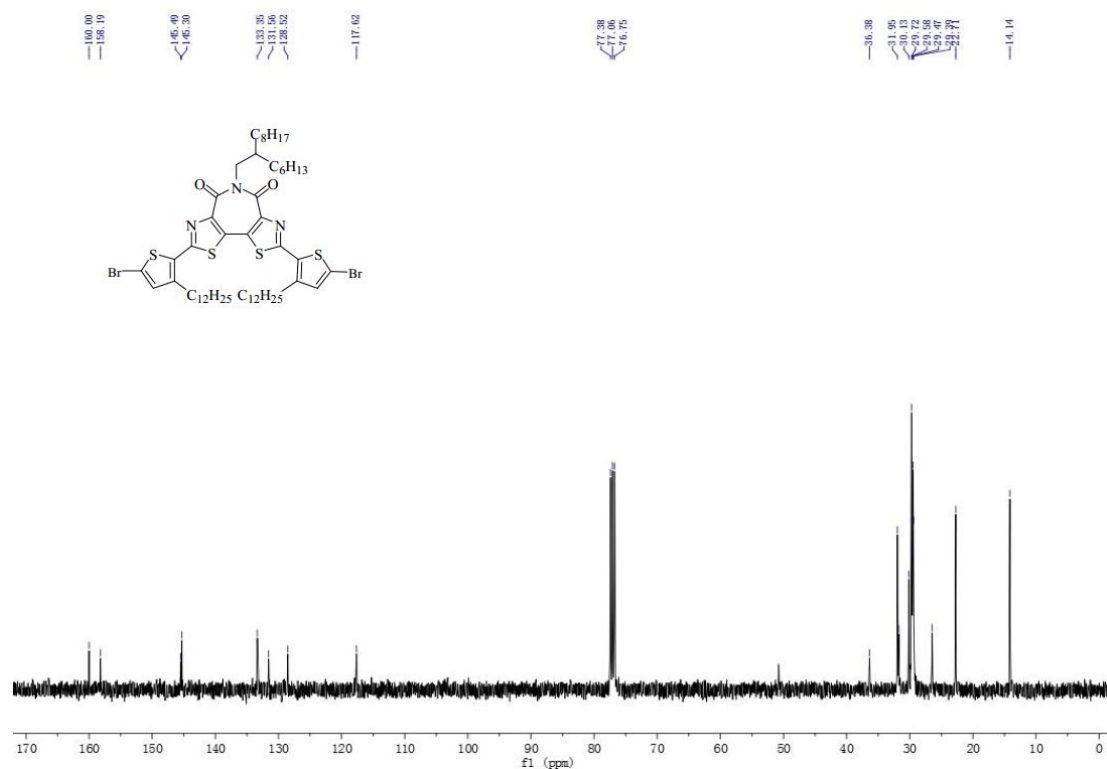


Figure S14. ^{13}C NMR spectrum of compound **10** (100 M, r.t., in CDCl_3).

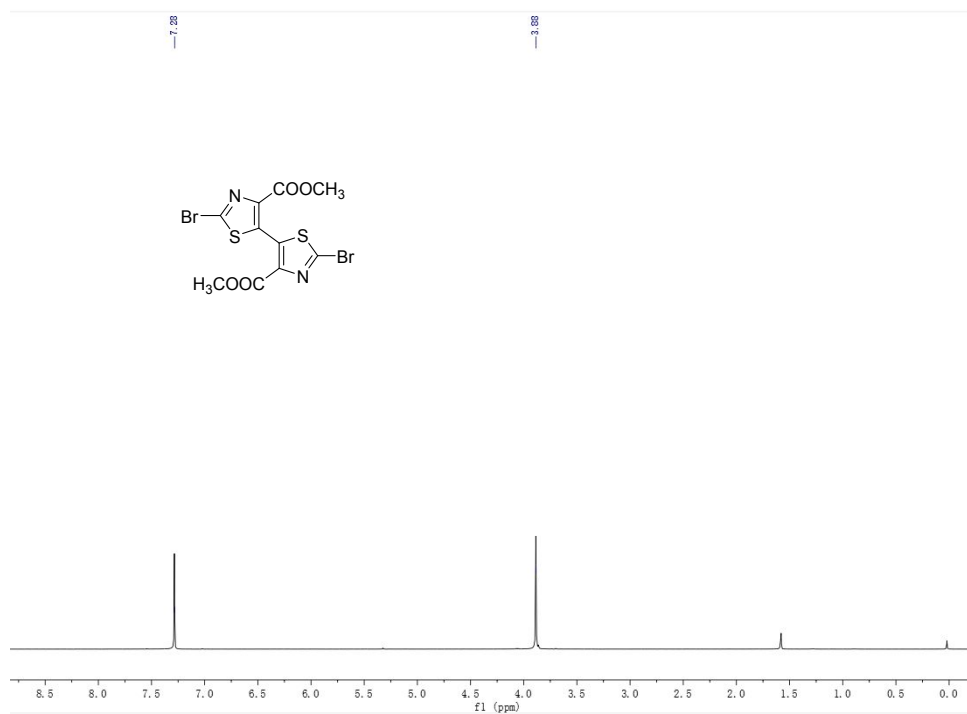


Figure S15. ^1H NMR spectrum of compound **12** (400 M, r.t., in CDCl_3).

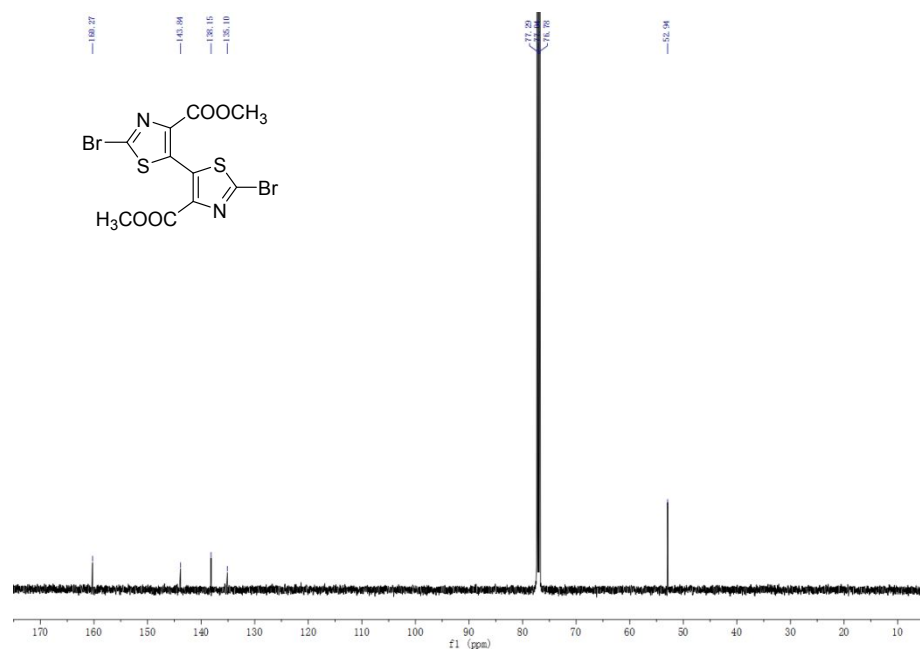


Figure S16. ¹³C NMR spectrum of compound **12** (400 M, r.t., in CDCl₃).

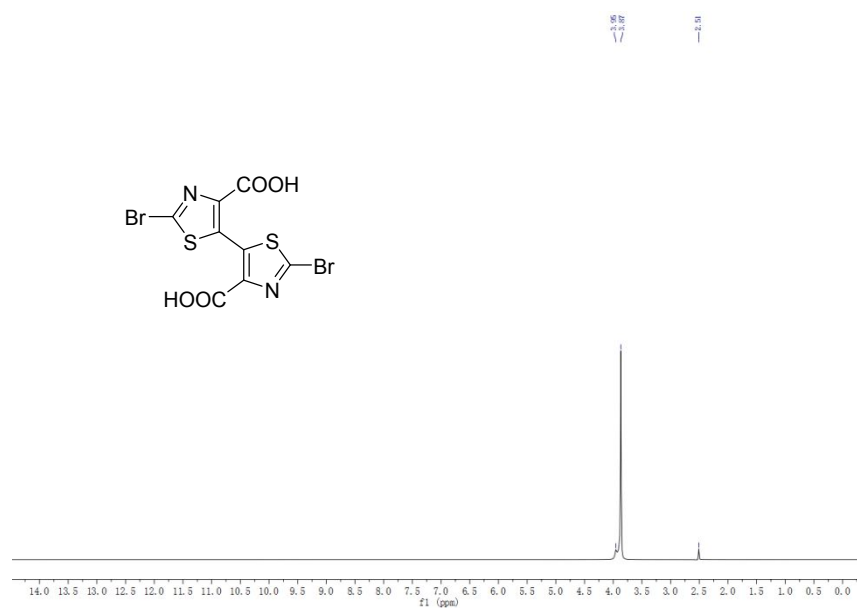


Figure S17. ¹H NMR spectrum of compound **13** (400 M, r.t., in DMSO).

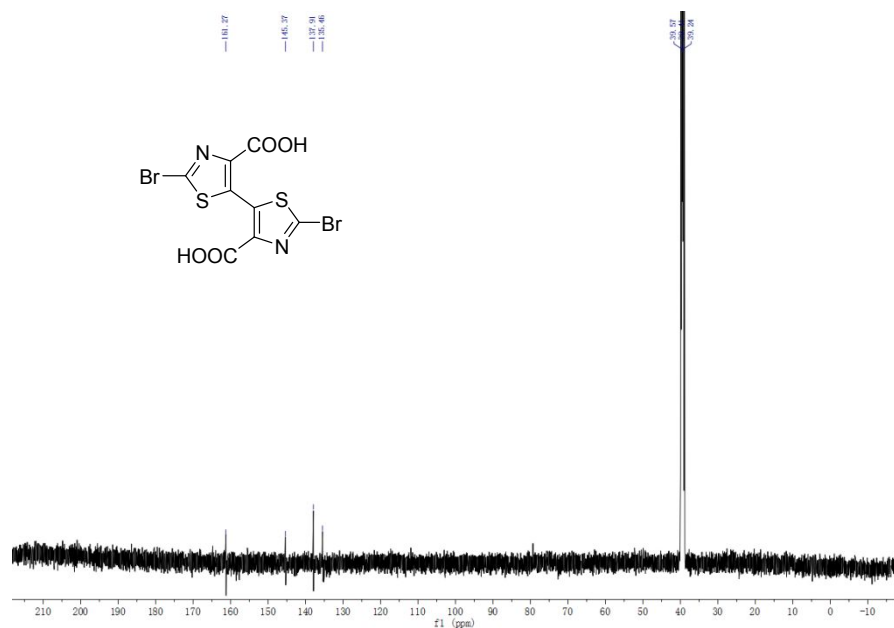


Figure S18. ^{13}C NMR spectrum of compound **13** (400 M, r.t., in DMSO).

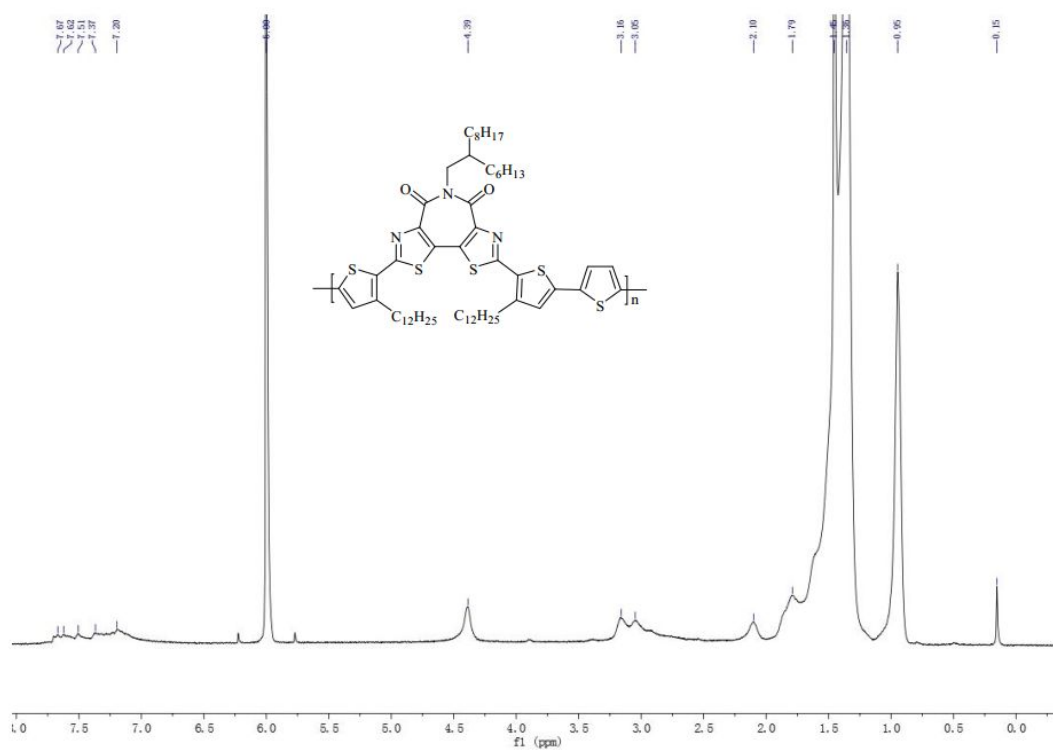


Figure S19. 1H NMR spectrum of polymer **PBTzI3T** (400 M, 120 °C, in $C_2Cl_4D_2$).

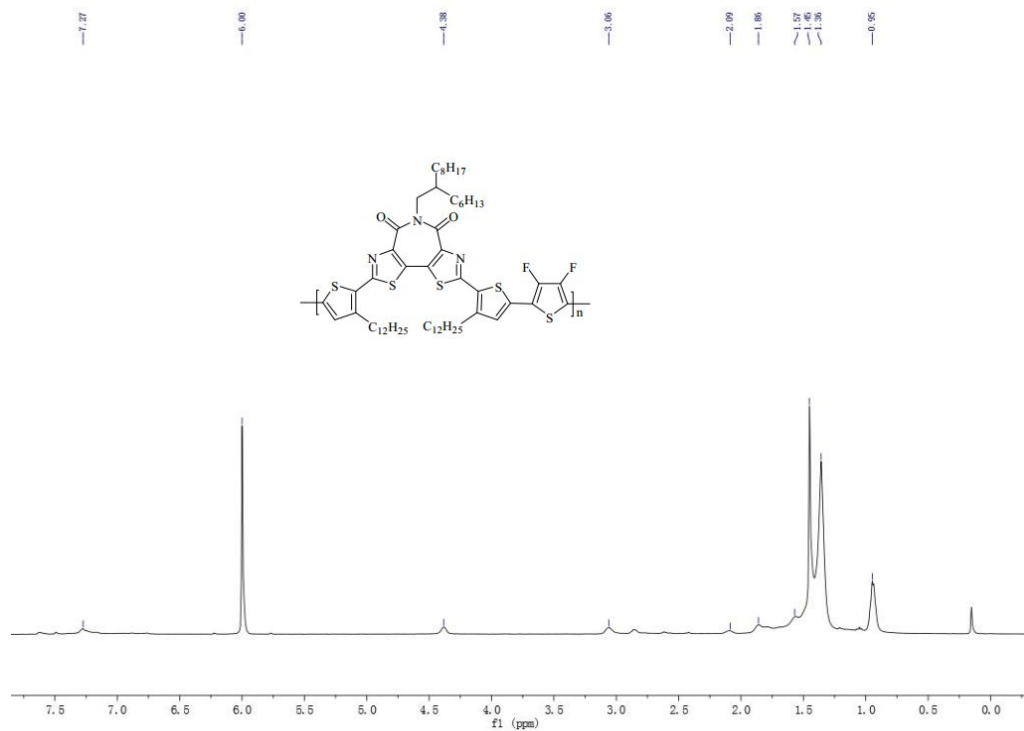


Figure S20. ^1H NMR spectrum of polymer **PBTzI3T-2F** (400 M, 120 $^\circ\text{C}$, in $\text{C}_2\text{Cl}_4\text{D}_2$).

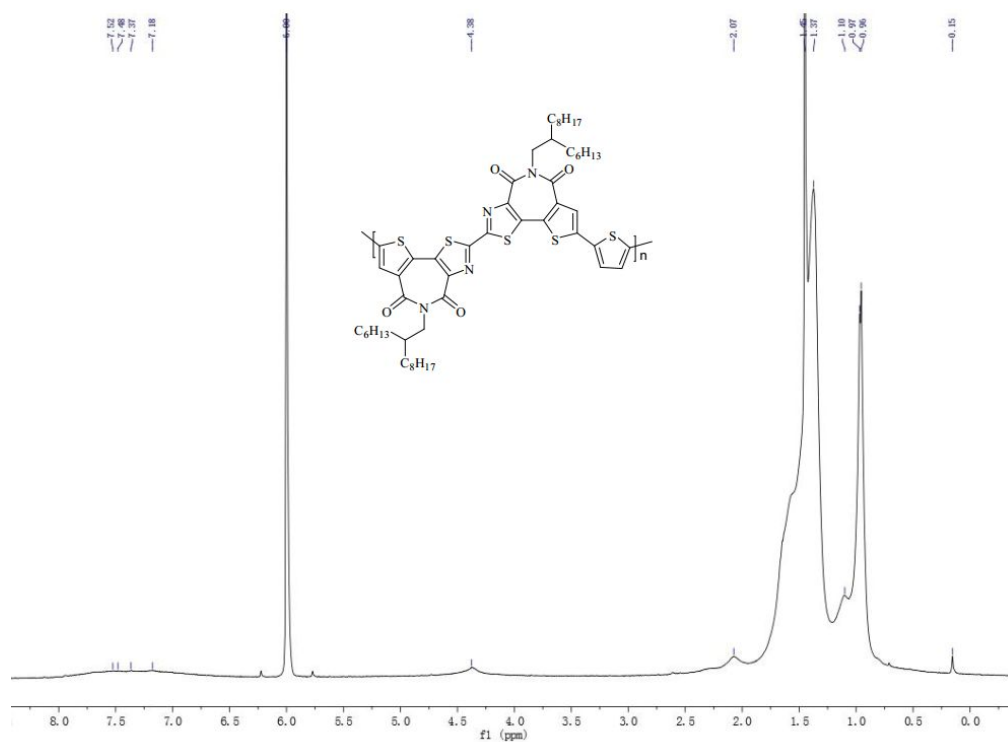


Figure S21. ^1H NMR spectrum of polymer **PDTzTIT** (400 M, 120 $^\circ\text{C}$, in $\text{C}_2\text{Cl}_4\text{D}_2$).

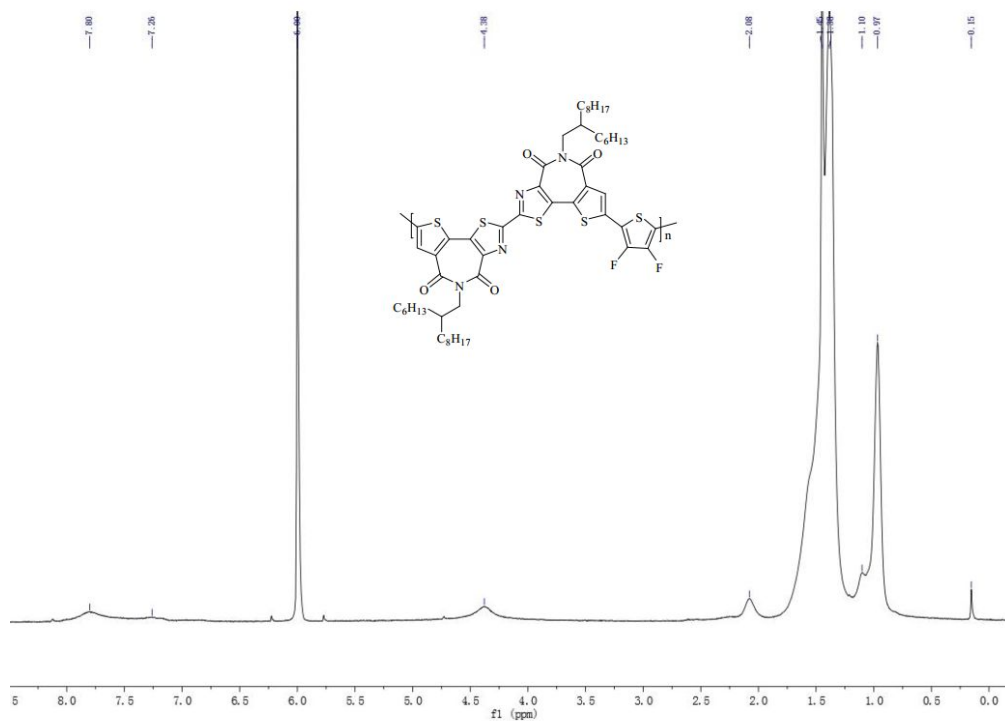


Figure S22. ^1H NMR spectrum of polymer **PDTzTIT-2F** (400 M, 120 °C, in $\text{C}_2\text{Cl}_4\text{D}_2$).

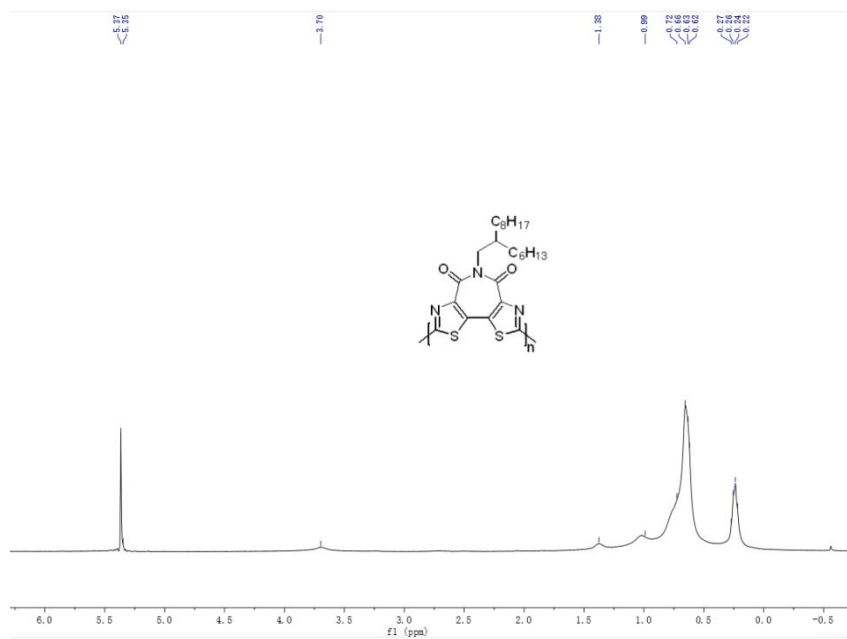
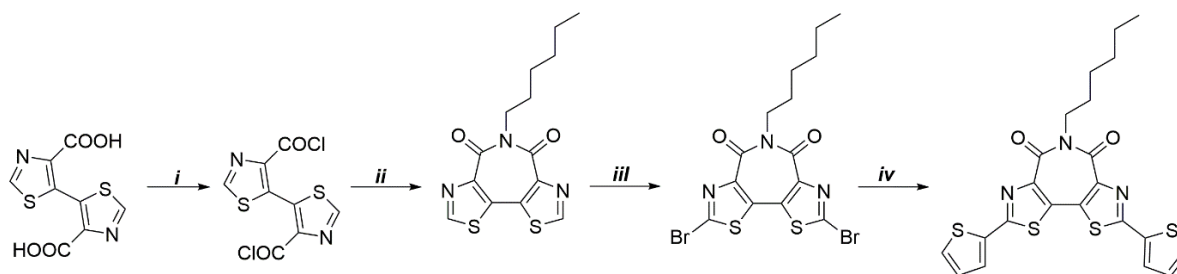


Figure S23. ^1H NMR spectrum of polymer **PBTzI** (400 M, 120 °C, in $\text{C}_2\text{Cl}_4\text{D}_2$).

4. Single Crystal Structure Data

Note: The cif file of the crystal structures of model compound is available free of charge via the internet at <http://www.ccdc.cam.ac.uk>

Scheme S1. Synthesis route to model compounds **BTzI-C6-2T** for single crystal structure study.



Reagents and conditions: (i) SOCl_2 , $80\text{ }^\circ\text{C}$; (ii) BTzI: *n*-hexylamine, $140\text{ }^\circ\text{C}$; (iii) LiHMDS, $\text{BrCCl}_2\text{CCl}_2\text{Br}$, $-78\text{ }^\circ\text{C}$; (iv) 2-(tributylstanny)thiophene, $\text{Pd}(\text{PPh}_3)_4$.

Computation details

Program(s) used to solve structure: *SHELXS97* (Sheldrick, 1990); program(s) used to refine structure: *SHELXL97* (Sheldrick, 1997).

Crystal data

CHNOS	$V = 13386(4) \text{ \AA}^3$
$M_r = 75.09$	$Z = 171$
	$F(000) = 6498$
$a = 46.450(6) \text{ \AA}$	$D_x = 1.593 \text{ Mg m}^{-3}$
$b = 46.450(6) \text{ \AA}$	Mo $K\alpha$ radiation, $\lambda = 0.71073 \text{ \AA}$
$c = 7.1640(14) \text{ \AA}$	$\mu = 0.76 \text{ mm}^{-1}$
$\alpha = 90^\circ$	$T = 566 \text{ K}$
$\beta = 90^\circ$	
$\gamma = 120^\circ$	

Data collection

Radiation source: fine-focus sealed tube	$R_{\text{int}} = 0.299$
graphite	$\theta_{\text{max}} = 25.3^\circ$, $\theta_{\text{min}} = 0.9^\circ$
67009 measured reflections	$h = -54 \rightarrow 55$
5433 independent reflections	$k = -55 \rightarrow 55$
3997 reflections with $I > 2\sigma(I)$	$l = -8 \rightarrow 8$

Refinement

Refinement on F^2	Secondary atom site location: difference Fourier map
Least-squares matrix: full	Hydrogen site location: inferred from neighbouring sites
$R[F^2 > 2\sigma(F^2)] = 0.112$	H atoms treated by a mixture of independent and constrained refinement
$wR(F^2) = 0.314$	$w = 1/[\sigma^2(F_o^2) + (0.1P)^2]$ where $P = (F_o^2 + 2F_c^2)/3$
$S = 1.66$	$(\Delta/\sigma)_{\text{max}} = 2.818$
5433 reflections	$\Delta_{\text{max}} = 0.49 \text{ e \AA}^{-3}$
290 parameters	$\Delta_{\text{min}} = -0.31 \text{ e \AA}^{-3}$
0 restraints	Extinction correction: <i>SHELXL</i> , $F_c^* = kF_c[1 + 0.001 \times F_c^2 \lambda^3 / \sin(2\theta)]^{-1/4}$
Primary atom site location: structure-invariant direct methods	Extinction coefficient: 0.0014 (3)

Special details

Geometry. All esds (except the esd in the dihedral angle between two l s. planes) are estimated using the full covariance matrix. The cell esds are taken into account individually in the estimation of esds in distances, angles, and torsion angles; correlations between esds in cell parameters are

only used when they are defined by crystal symmetry. An approximate (isotropic) treatment of cell esds is used for estimating esds involving l.s. planes.

Refinement. Refinement of F^2 against ALL reflections. The weighted R-factor wR and goodness of fit S are based on F^2 , conventional R-factors R are based on F, with F set to zero for negative F^2 . The threshold expression of $F^2 > 2\sigma(F^2)$ is used only for calculating R-factors(gt) etc. and is not relevant to the choice of reflections for refinement. R-factors based on F^2 are statistically about twice as large as those based on F, and R- factors based on ALL data will be even larger.

Fractional atomic coordinates and isotropic or equivalent isotropic displacement parameters (\AA^2)

	<i>x</i>	<i>y</i>	<i>z</i>	$U_{\text{iso}}^*/U_{\text{eq}}$
S1	0.59118 (3)	0.02945 (3)	0.48137 (16)	0.1017 (5)
S2	0.56552 (4)	0.04816 (4)	0.10957 (17)	0.1071 (5)
S3	0.52163 (3)	0.04637 (4)	-0.43368 (18)	0.1115 (6)
S4	0.61358 (4)	-0.02205 (4)	0.9175 (2)	0.1117 (5)
N1	0.57958 (10)	-0.02973 (11)	0.5368 (6)	0.0994 (11)
C2	0.56421 (11)	-0.03041 (13)	0.3706 (7)	0.0963 (13)
C3	0.59447 (12)	-0.00046 (13)	0.6085 (6)	0.0943 (12)
C4	0.61225 (12)	0.00807 (13)	0.7864 (7)	0.0988 (13)
C5	0.64290 (12)	0.03715 (16)	1.0492 (7)	0.1104 (16)
C6	0.62999 (11)	0.04061 (14)	0.8695 (6)	0.0954 (13)
C7	0.63596 (13)	0.00551 (14)	1.0881 (7)	0.1066 (14)
C8	0.53800 (11)	-0.01219 (14)	0.0062 (6)	0.0981 (13)
N9	0.53222 (10)	0.00361 (14)	-0.1365 (5)	0.1065 (12)
C10	0.55610 (11)	0.00791 (13)	0.1520 (6)	0.0960 (13)
C11	0.54532 (13)	0.03557 (16)	-0.1026 (7)	0.1045 (14)
C12	0.56771 (11)	-0.00074 (12)	0.3187 (6)	0.0925 (12)
C13	0.52358 (15)	-0.04809 (17)	-0.0143 (8)	0.1182 (17)
N14	0.52841 (12)	-0.06914 (12)	0.1089 (7)	0.1202 (14)
O15	0.50594 (13)	-0.06166 (12)	-0.1488 (7)	0.1577 (17)
C16	0.54349 (14)	0.05878 (17)	-0.2297 (7)	0.1133 (16)
O17	0.55063 (12)	-0.08532 (11)	0.3344 (7)	0.1488 (16)
C18	0.51183 (18)	-0.10410 (16)	0.0468 (11)	0.154 (3)
C19	0.54813 (14)	-0.06232 (16)	0.2712 (8)	0.1166 (16)
C20	0.53291 (18)	0.08649 (17)	-0.4873 (9)	0.1337 (19)
C21	0.5589 (2)	0.09301 (18)	-0.2097 (9)	0.147 (2)
C22	0.5517 (2)	0.10770 (19)	-0.3587 (10)	0.169 (3)
C23	0.5360 (2)	-0.1077 (2)	-0.0991 (14)	0.177 (3)
C32	0.5412 (4)	-0.1485 (4)	-0.317 (2)	0.288 (8)
C33	0.5164 (3)	-0.1442 (3)	-0.1917 (19)	0.229 (5)

C34	0.5206 (7)	-0.1863 (8)	-0.411 (4)	0.352 (13)
C35	0.4823 (6)	-0.2282 (7)	-0.692 (4)	0.502 (16)
C36	0.5044 (7)	-0.1861 (7)	-0.556 (5)	0.374 (14)

Atomic displacement parameters (\AA^2)

	U^{11}	U^{22}	U^{33}	U^{12}	U^{13}	U^{23}
S1	0.1142 (9)	0.1227 (10)	0.0766 (7)	0.0655 (8)	-0.0023 (6)	0.0077 (6)
S2	0.1189 (10)	0.1289 (10)	0.0794 (8)	0.0663 (8)	-0.0030 (6)	0.0090 (6)
S3	0.1138 (10)	0.1369 (12)	0.0850 (8)	0.0636 (8)	-0.0021 (6)	0.0109 (7)
S4	0.1118 (10)	0.1248 (11)	0.0962 (9)	0.0572 (8)	-0.0030 (7)	0.0191 (7)
N1	0.093 (2)	0.112 (3)	0.092 (2)	0.050 (2)	0.0008 (19)	0.010 (2)
C2	0.087 (3)	0.110 (3)	0.087 (3)	0.046 (3)	0.000 (2)	0.012 (3)
C3	0.092 (3)	0.114 (4)	0.081 (3)	0.055 (3)	0.007 (2)	0.015 (2)
C4	0.088 (3)	0.126 (4)	0.088 (3)	0.058 (3)	0.006 (2)	0.016 (3)
C5	0.094 (3)	0.149 (5)	0.082 (3)	0.056 (3)	0.007 (2)	0.004 (3)
C6	0.085 (3)	0.133 (4)	0.070 (2)	0.056 (3)	0.004 (2)	0.006 (2)
C7	0.101 (3)	0.125 (4)	0.088 (3)	0.052 (3)	0.000 (2)	0.016 (3)
C8	0.089 (3)	0.122 (4)	0.080 (3)	0.050 (3)	0.002 (2)	0.011 (3)
N9	0.094 (2)	0.144 (4)	0.079 (2)	0.058 (3)	0.0022 (19)	0.015 (2)
C10	0.093 (3)	0.122 (3)	0.074 (2)	0.055 (3)	0.003 (2)	0.009 (2)
C11	0.097 (3)	0.130 (4)	0.080 (3)	0.052 (3)	0.005 (2)	0.010 (3)
C12	0.088 (3)	0.114 (3)	0.077 (3)	0.052 (2)	0.004 (2)	0.010 (2)
C13	0.112 (4)	0.142 (5)	0.096 (3)	0.059 (4)	-0.017 (3)	0.002 (3)
N14	0.118 (3)	0.117 (3)	0.109 (3)	0.047 (3)	-0.023 (3)	0.002 (3)
O15	0.182 (4)	0.156 (4)	0.127 (3)	0.078 (3)	-0.058 (3)	-0.015 (3)
C16	0.115 (4)	0.142 (5)	0.077 (3)	0.060 (3)	0.005 (2)	0.020 (3)
O17	0.157 (4)	0.117 (3)	0.162 (4)	0.060 (3)	-0.043 (3)	0.010 (3)
C18	0.143 (5)	0.106 (4)	0.171 (6)	0.030 (4)	-0.048 (5)	-0.010 (4)
C19	0.108 (4)	0.117 (4)	0.109 (4)	0.045 (3)	-0.013 (3)	0.006 (3)
C20	0.151 (5)	0.141 (5)	0.102 (4)	0.068 (4)	-0.013 (4)	0.017 (4)
C21	0.184 (6)	0.125 (5)	0.106 (4)	0.058 (4)	-0.038 (4)	0.019 (3)
C22	0.208 (7)	0.131 (5)	0.127 (5)	0.054 (5)	-0.043 (5)	0.017 (4)
C23	0.181 (7)	0.150 (6)	0.200 (8)	0.082 (5)	-0.035 (6)	-0.059 (6)
C32	0.303 (17)	0.229 (12)	0.309 (17)	0.115 (12)	0.015 (14)	-0.117 (12)
C33	0.222 (10)	0.169 (8)	0.262 (13)	0.071 (7)	-0.045 (9)	-0.076 (8)
C34	0.35 (3)	0.39 (3)	0.34 (3)	0.20 (3)	-0.01 (2)	-0.04 (3)
C35	0.36 (2)	0.43 (3)	0.55 (3)	0.08 (2)	0.21 (2)	-0.15 (3)
C36	0.39 (3)	0.31 (2)	0.41 (3)	0.17 (2)	-0.04 (3)	0.01 (2)

Geometric parameters (\AA , $^\circ$)

S1—C3	1.731 (5)	C8—C13	1.461 (8)
S1—C12	1.728 (5)	N9—C11	1.315 (7)
S2—C10	1.721 (5)	C10—C12	1.447 (6)
S2—C11	1.728 (5)	C11—C16	1.446 (8)
S3—C20	1.708 (7)	C13—O15	1.217 (6)
S3—C16	1.707 (5)	C13—N14	1.416 (7)
S4—C4	1.712 (5)	N14—C19	1.415 (7)

S4—C7	1.698 (6)	N14—C18	1.476 (8)
N1—C3	1.285 (6)	C16—C21	1.387 (9)
N1—C2	1.380 (6)	O17—C19	1.218 (7)
C2—C12	1.356 (7)	C18—C23	1.603 (12)
C2—C19	1.468 (8)	C20—C22	1.312 (9)
C3—C4	1.462 (7)	C21—C22	1.393 (9)
C4—C6	1.440 (7)	C23—C33	1.610 (12)
C5—C7	1.367 (8)	C32—C33	1.550 (19)
C5—C6	1.462 (7)	C32—C34	1.67 (3)
C8—C10	1.373 (7)	C34—C36	1.29 (3)
C8—N9	1.361 (6)	C35—C36	1.95 (4)
C3—S1—C12	88.7 (2)	C16—C11—S2	121.8 (5)
C10—S2—C11	89.3 (3)	C2—C12—C10	129.5 (5)
C20—S3—C16	91.0 (3)	C2—C12—S1	110.2 (3)
C4—S4—C7	92.1 (3)	C10—C12—S1	120.2 (4)
C3—N1—C2	111.6 (4)	O15—C13—C8	118.5 (5)
C12—C2—N1	114.5 (5)	O15—C13—N14	115.7 (6)
C12—C2—C19	129.4 (5)	C8—C13—N14	125.8 (5)
N1—C2—C19	115.9 (5)	C19—N14—C13	131.8 (5)
N1—C3—C4	124.6 (4)	C19—N14—C18	114.7 (5)
N1—C3—S1	115.0 (4)	C13—N14—C18	113.3 (5)
C4—C3—S1	120.4 (4)	C11—C16—C21	126.9 (5)
C6—C4—C3	126.5 (4)	C11—C16—S3	122.3 (5)
C6—C4—S4	113.3 (4)	C21—C16—S3	110.7 (4)
C3—C4—S4	120.2 (4)	N14—C18—C23	107.7 (6)
C7—C5—C6	114.1 (5)	O17—C19—N14	116.3 (5)
C4—C6—C5	107.4 (5)	O17—C19—C2	118.8 (5)
C5—C7—S4	113.0 (4)	N14—C19—C2	124.8 (5)
C10—C8—N9	115.0 (5)	C22—C20—S3	112.7 (5)
C10—C8—C13	128.9 (4)	C16—C21—C22	111.7 (6)
N9—C8—C13	116.0 (5)	C20—C22—C21	113.8 (7)
C11—N9—C8	111.4 (4)	C18—C23—C33	108.7 (8)
C8—C10—C12	128.7 (5)	C33—C32—C34	107.4 (15)
C8—C10—S2	109.9 (3)	C32—C33—C23	107.8 (10)
C12—C10—S2	121.3 (4)	C36—C34—C32	111 (3)
N9—C11—C16	124.0 (5)	C34—C36—C35	114 (3)
N9—C11—S2	114.3 (4)		

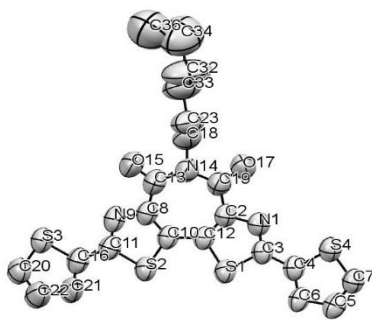


Figure S24. X-ray crystallographic structure of the model compound **BTzI-C6-2T**.

5. Polymer Thermal Properties.

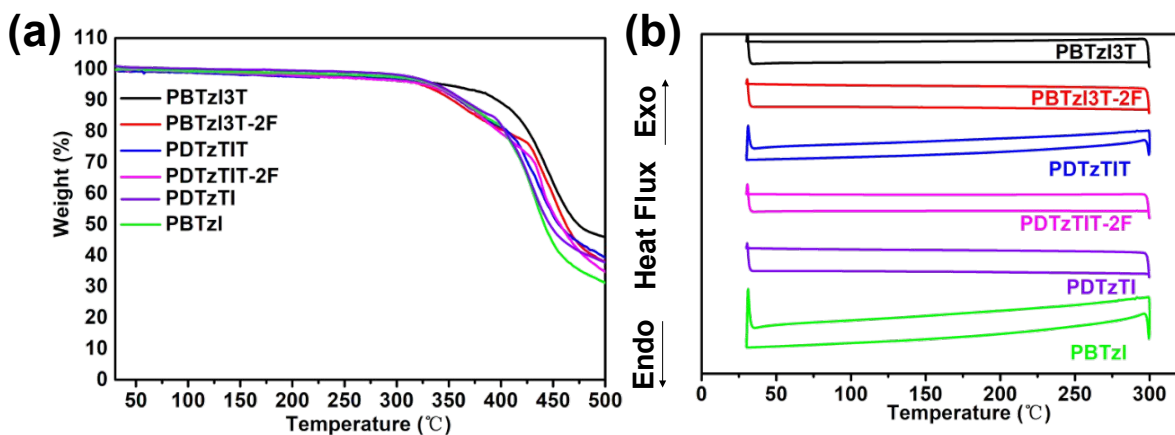


Figure S25. (a) Thermogravimetric analysis of polymers **PBTzI3T**, **PBTzI3T-2F**, **PDTzTIT**, **PDTzTIT-2F**, **PDTzTI**, and **PBTzI** at a heating rate of $10\text{ }^{\circ}\text{C min}^{-1}$. (b) DSC thermograms of polymers **PBTzI3T**, **PBTzI3T-2F**, **PDTzTIT**, **PDTzTIT-2F**, **PDTzTI**, and **PBTzI**. The DSC curves are from the second heating and first cooling scans with a ramp rate of $10\text{ }^{\circ}\text{C min}^{-1}$. N_2 was used as the purge gas for both TGA and DSC measurements.

6. Polymer Optical and Electrochemical Properties.

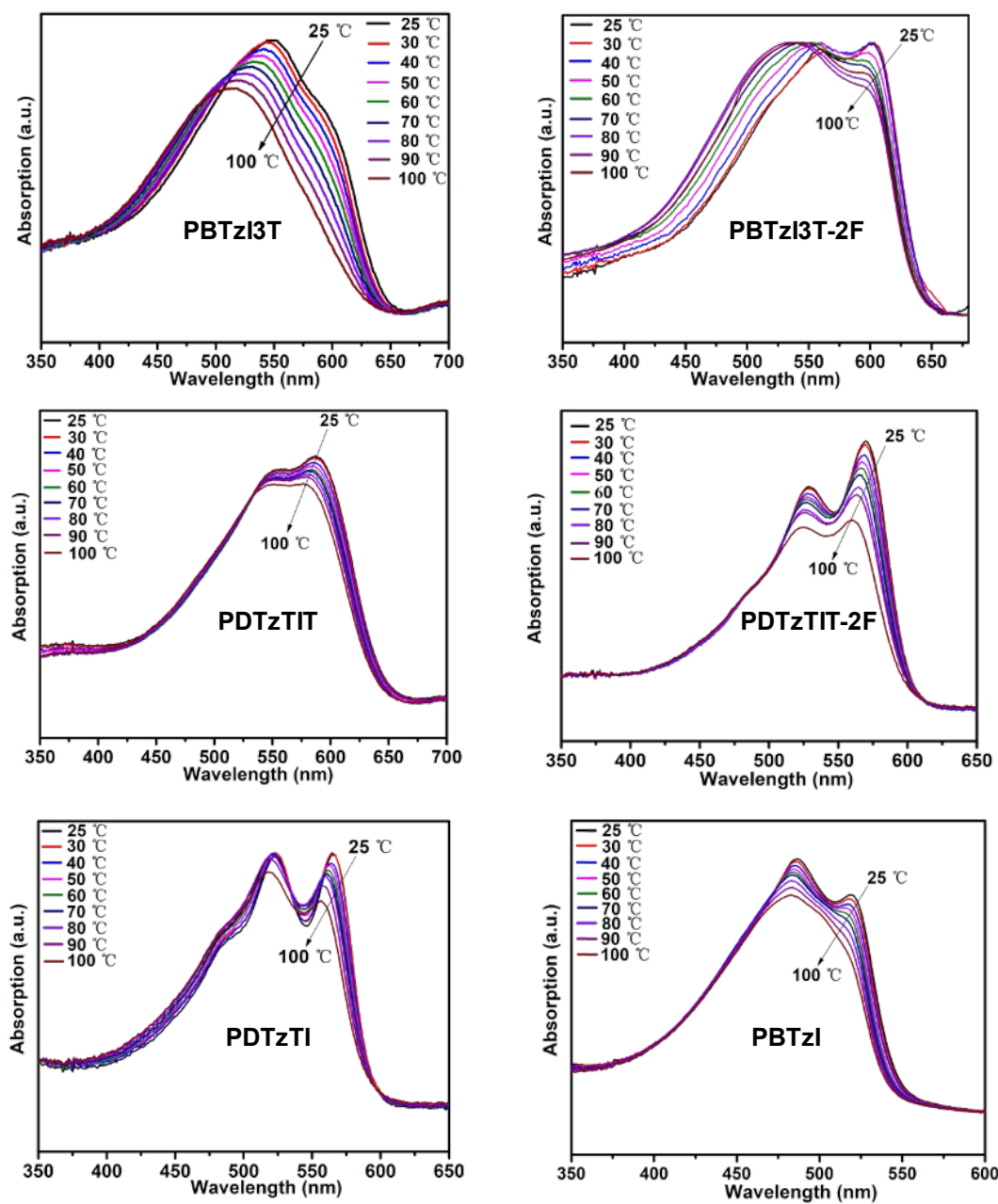


Figure S26. Temperature-dependent UV-vis absorption of polymers **PBTzI3T**, **PBTzI3T-2F**, **PDTzTIT**, **PDTzTIT-2F**, **PDTzTI**, and **PBTzI** in diluted chlorobenzene solution (10^{-5} M).

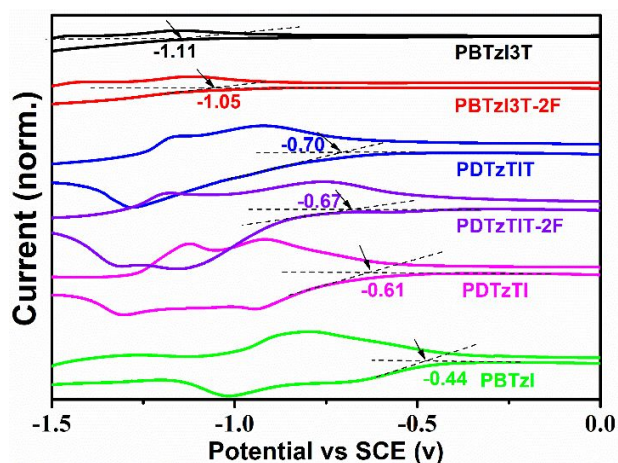


Figure S27. Cyclic voltammograms of polymer thin films measured in 0.1 M tetrabutyl ammonium hexafluorophosphate acetonitrile solutions with the Fc/Fc^+ redox couple as the internal standard at a scanning rate of 50 mV s^{-1} .

7. OTFT Fabrication and Characterization.

Top-gate/bottom-contact (TG/BC) configuration was used for organic thin-film transistors (OTFTs). The source and drain electrodes (30 nm Au with 3 nm Cr adhesion layer) were patterned on borosilicate glass by standard photolithography process. The patterned glass substrates were cleaned by sonication in acetone and isopropanol for 10 min each, followed by UV-ozone treatment for 30 min. The cleaned substrates were transferred into a N_2 -filled glove box (O_2 , H_2O concentration $< 0.1 \text{ ppm}$) for the following steps. The semiconductor layer was spin-coated from hot chlorobenzene or 1,2-dichlorobenzene solution (5 mg mL^{-1}), then annealed at various temperatures for 10 or 30 min followed by cooling down process. The dielectric layer was spin-coated from either poly(methyl methacrylate) solution (PMMA, Sigma Aldrich, average M_w 120k, 60 mg mL^{-1} in *n*-butyl acetate) or diluted CYTOP solutions (CTL-809M:CT-SOLV180 = 2:1, volume ratio, Asahi Glass Co., Ltd.), then annealed at 100°C for 30 min, the thickness of the

dielectric layer is 500 nm for PMMA and 400 nm for CYTOP. Finally, 50 nm Aluminum was thermally evaporated on top under a high vacuum ($< 10^{-6}$ Torr) as the gate electrode.

For off-center spin-coated device, the patterned substrates were cleaned following the same manner as above. For the off-center spin-coating process, the substrates were fixed onto glass slide and placed at a distance of ~ 3 cm from the center of spin-coater. The semiconductor layer was spin-coated from hot solution (mixed solvent, chlorobenzene:1,2-dichlorobenzene = 3:1, volume ratio, 5 mg mL⁻¹), then annealed for 20 min followed by cooling down process. Finally, the CYTOP dielectric layer and Al gate electrode were deposited following the same procedure as above to finish device fabrication. Additionally, zinc oxide (ZnO) was used as electron injection layer for PDTzTI off center spin-coated device, which was spin-casted in clean room ambient environment then annealed at 200 °C for 30 min following published procedure.⁴

The field-effect transistor devices were measured in a N₂-filled glove box using Keithley S4200 SCS semiconductor characterization system. The saturation field-effect mobility was calculated from the average slope of the $|I_s|^{1/2}$ vs V_g plots in the high V_g region (70–80 V) to avoid mobility overestimation.

Table S1. TG/BC OTFT performance parameters of **PBTzI3T**, **PBTzI3T-2F**, **PDTzTIT**, **PDTzTIT-2F**, **PDTzTI**, and **PBTzTI** fabricated with conventional on-center spin-coating method and annealed under various temperatures.

Polymer	Dielectric	T_{anneal} (°C)	μ_e (cm ² V ⁻¹ s ⁻¹) ^a	μ_h (cm ² V ⁻¹ s ⁻¹) ^a	V_T (V) ^b	$I_{\text{on}}/I_{\text{off}}$
PBTzI3T	CYTOP	r.t.	0.012 (0.008)	2.4×10^{-4}	n: 49	n: 10 ³ -10 ⁴
		150	0.012 (0.01)	2.9×10^{-4}	n: 53	n: 10 ³ -10 ⁴
		200	0.02 (0.012)	1.9×10^{-4}	n: 52	n: 10 ³ -10 ⁴
PBTzI3T-2F	PMMA	150	0.05 (0.04)	2.4×10^{-4}	n: 53	n: 10 ⁴ -10 ⁵
		200	0.05 (0.037)	3.1×10^{-4}	n: 53	n: 10 ⁴ -10 ⁵
PDTzTIT	CYTOP	r.t.	0.10 (0.07)	NA	n: 50	n: 10 ⁵ -10 ⁶
		150	0.11 (0.08)	NA	n: 45	n: 10 ⁵ -10 ⁶
		200	0.13 (0.11)	NA	n: 46	n: 10 ⁵ -10 ⁶
PDTzTIT-2F	CYTOP	r.t.	0.40 (0.3)	NA	n: 38	n: 10 ⁶ -10 ⁷
		150	0.56 (0.38)	NA	n: 37	n: 10 ⁶ -10 ⁷
		250	0.40 (0.27)	NA	n: 41	n: 10 ⁶ -10 ⁷
		300	0.35 (0.26)	NA	n: 43	n: 10 ⁶ -10 ⁷
PDTzTI	CYTOP	r.t.	0.16 (0.10)	NA	n:48	n: 10 ⁶ -10 ⁷
		150	0.79 (0.62)	NA	n:42	n: 10 ⁷ -10 ⁸
		250	0.50 (0.37)	NA	n:44	n: 10 ⁶ -10 ⁷
		300	0.33 (0.30)	NA	n:47	n: 10 ⁶ -10 ⁷
PBTzTI	CYTOP	r.t.	4.9×10^{-3} (4.4×10^{-3})	NA	n: 25	n: 10 ⁵ -10 ⁶
		100	6.1×10^{-3} (5.0×10^{-3})	NA	n: 26	n: 10 ⁵ -10 ⁶
		150	7.2×10^{-3} (6.6×10^{-3})	NA	n: 28	n: 10 ⁵ -10 ⁶
		200	8.9×10^{-3} (8.1×10^{-3})	NA	n: 28	n: 10 ⁵ -10 ⁶
		300	0.010 (8.0×10^{-3})	NA	n: 34	n: 10 ⁵ -10 ⁶

^a Maximum mobilities from at least 5 devices (average value shown in parentheses); ^b Average threshold values shown.

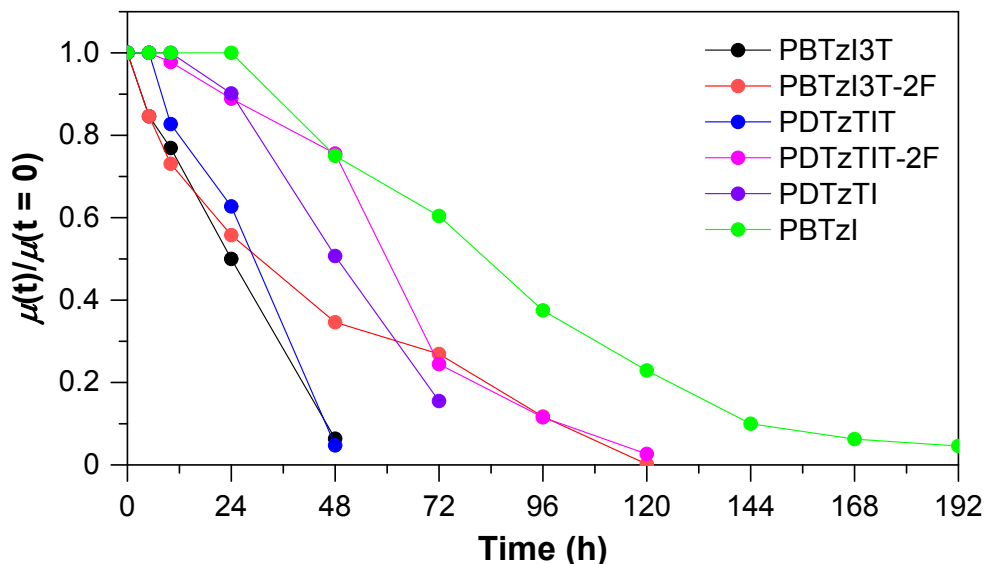


Figure S28. Temporal evolution of device performance of TG/BC OTFTs fabricated with imide-functionalized thiazole-based polymer semiconductors. The transistors were stored in ambient air having a relative humidity around 50% without any special encapsulation. The electron mobility values were normalized to the mobility at the beginning of the test for easier comparison.

8. GIWAXS Measurements and Data.

GIWAXS measurements were conducted at 23A SWAXS beamline at the National Synchrotron Radiation Research Center, Hsinchu, Taiwan with a 10 keV primary beam, 0.15° incident angle and C9728DK area detector. The films are prepared under the same conditions for the best-performing OTFT devices, but on silicon substrates.

Table S2. Peak positions, d-spacings, and crystal coherence lengths of polymer films of **PBTzI3T**, **PBTzI3T-2F**, **PDTzTIT**, **PDTzTIT-2F**, **PDTzTI**, and **PBTzI** fabricated under the optimal conditions for OTFT devices, which were calculated via Scherrer equation.

Polymer	lamellar peak			π - π stacking peak		
	peak position (\AA^{-1})	d-spacing (\AA)	crystal coherence length (nm)	peak position (\AA^{-1})	d-spacing (\AA)	crystal coherence length (nm)
PBTzI3T	0.286	22.0	15.9	1.75	3.59	5.01
PBTzI3T-2F	0.282	22.3	13.4	1.75	3.59	4.25
PDTzTIT	0.291	21.6	12.3	1.74	3.61	4.13
PDTzTIT-2F	0.288	21.8	14.8	1.73	3.63	4.04
PDTzTI	0.284	22.1	16.1	1.72	3.65	4.38
PBTzI	0.260	24.2	8.70	1.74	3.61	11.93

References:

- (1) Getmanenko, Y. A.; Tongwa, P.; Timofeeva, T. V.; Marder, S. R., Base-Catalyzed Halogen Dance Reaction and Oxidative Coupling Sequence as a Convenient Method for the Preparation of Dihalo-bisheteroarenes. *Org. Lett.* **2010**, *12*, 2136-2139.
- (2) Stangeland, E. L.; Sammakia, T., Use of Thiazoles in the Halogen Dance Reaction: Application to the Total Synthesis of WS75624 B. *J. Org. Chem.* **2004**, *69*, 2381-2385.
- (3) Saito, M.; Osaka, I.; Suda, Y.; Yoshida, H.; Takimiya, K., Dithienylthienothiophenebisimide, a Versatile Electron-Deficient Unit for Semiconducting Polymers. *Adv. Mater.* **2016**, *28*, 6921-6925.
- (4) Sun, Y.; Seo, J. H.; Takacs, C. J.; Seifert, J.; Heeger, A. J., Inverted Polymer Solar Cells Integrated with a Low-Temperature-Annealed Sol-Gel-Derived ZnO Film as an Electron Transport Layer. *Adv. Mater.* **2011**, *23*, 1679-1683.